2009

Seismic Energy Dissipation of Steel Buildings Using Engineered Cladding Systems

Quan Viet Nguyen
University of Massachusetts Amherst, nvquan@gmail.com

SEISMIC ENERGY DISSIPATION OF BUILDINGS USING ENGINEERED CLADDING SYSTEMS

A Thesis Presented

by

QUAN VIET NGUYEN

Submitted to the Graduate School of the
University of Massachusetts Amherst in partial fulfillment
of the requirements for the degree of

MASTER OF SCIENCE IN CIVIL ENGINEERING

May 2009

Civil and Environmental Engineering

SEISMIC ENERGY DISSIPATION OF BUILDINGS USING ENGINEERED CLADDING SYSTEMS

A Thesis Presented

by

QUAN VIET NGUYEN

Approved as to style and content by:

_____
Scott A. Civjan, Chair

_____
Sanjay R. Arwade, Member

_____
Sergio F. Breña, Member

_____
Richard N. Palmer
Graduate Program Director
Civil and Environmental Engineering Department

ACKNOWLEDGMENTS

First and foremost, I would like to express my deep appreciation to my advisor, Dr. Scott A. Civjan, for his original idea of this research and continued guidance and support during my Master's studies at the University of Massachusetts Amherst. Without his help this thesis would not be possible and I myself would never be where I am today.

I would like to thank Dr. Sergio F. Breña and Dr. Sanjay R. Arwade for serving on my research committee and providing insightful comments on the final draft of this thesis.

I would also like to thank Dr. Thomas J. Lardner for his stimulating lectures on structural dynamics and structural stability.

Lastly, but most importantly, thank you to the members of my family for their unending support and encouragement over the years. I dedicate this work to them.

TABLE OF CONTENTS

Page

LIST OF TABLES

LIST OF FIGURES

CHAPTER 1

INTRODUCTION

1.1 Overview

Precast concrete claddings have been widely used in the United States since the 1920s. Cladding panels are attached to the frame structures and function as the facades of buildings (Fig. 1.1). Advantages of precast facade include a wide variety of styles, shapes and sizes, long-term durability that requires low maintenance over time and fast speed of erection that helps to reduce overall project cost. The *PCI Architectural Precast Concrete Manual* (Precast/Prestressed 2007), which is an industry guideline on the design of precast cladding elements for architects and engineers, provides an excellent overview of cladding systems. A brief review of these concepts are presented in Section 1.2.

This research examines the seismic energy dissipation potential of steel structures by focusing on new types of specially engineered cladding-to-frame connections. Traditional connection details consist of rigid restraint of cladding panels, resulting in seismic designs that only consider the panel self-weight with the connection design left up to the precast fabricators and typical details. Beyond this, no contribution of the cladding panels to the behavior of a structure is considered. It is postulated that by considering these elements to actively participate in building response a more efficient and resilient structure could be designed which accurately captures the effects of non-structural cladding elements on building behavior.

There has been limited research studying the interaction between cladding systems and the structural frame during seismic events (Goodno & Palsson 1986, Henry & Roll 1986, Cohen & Powel 1993). It has been shown that if properly designed for

seismic loads, the cladding system may have the ability to dissipate energy, resulting in a reduction of structural responses under earthquakes (Pinelli et al. 1995). However, Pinelli et al. (1995) was focused on one building with a specific connection design. A revisiting of these concepts in the context of a general approach to structural design is warranted.

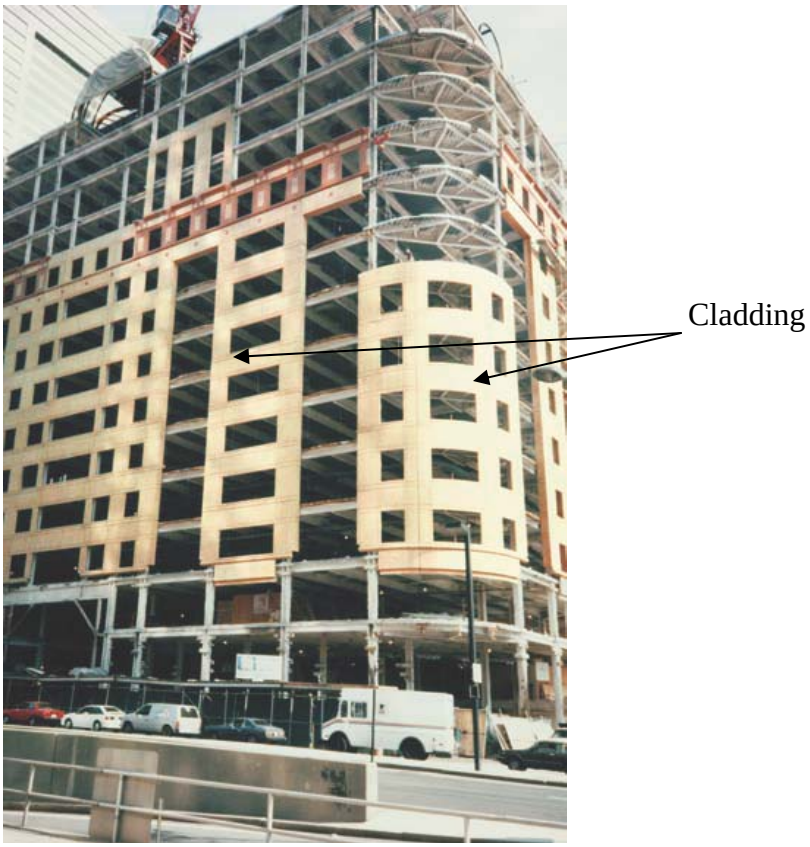

Figure 1.1 Building using cladding system (from Precast/Prestressed 2007, by permission).

1.2 Current connection practice

Cladding systems are divided by individual units (Fig. 1.2). Normally, the height of a panel unit does not exceed the floor-to-floor height, and the width of a panel unit does not exceed the building bay width. Panel geometry and joints must be configured

such that panels do not bear on one another and do not collide with one another or with the supporting structure during a seismic event or due to moisture or temperature effects.

Cross-sections of typical wall claddings are shown in Figure 1.3. Basically, a cladding panel consists of an outer layer of concrete facing outside of the building, an intermediate insulation layer and an inner wallboard layer facing the inside of the building. The concrete layer contributes the most to the weight of the cladding panel.

Figure 1.2 Cladding units (from Precast/Prestressed 2007, by permission).

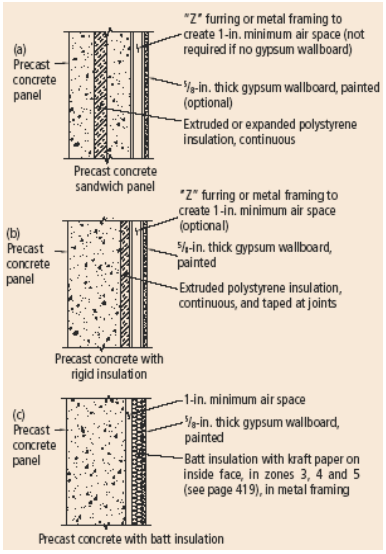

Figure 1.3 Typical cross-sections of cladding panels (from Precast/Prestressed 2007, by permission).

Cladding panels are attached to the frame structures through connections. Panel attachment typically consists of two bearing connections and two lateral (or tieback)

connections (Fig. 1.4). Details of one specific type of both a bearing and tieback connection are shown in Figure1.5 and 1.6. Bearing connections are intended to transfer vertical loads to the support structure or foundation. Tieback connections are primarily intended to keep the precast concrete unit in vertical configuration and to resist wind and seismic loads perpendicular (out-of-plane) to the panel. They are designed to deform under lateral forces in the plane of the panel with minimal resistance.

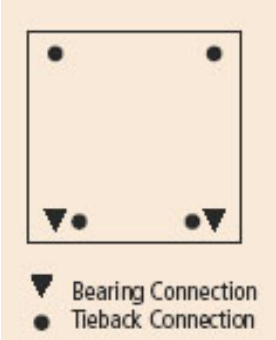

Figure 1.4 Typical connections arrangement (from Precast/Prestressed 2007, by permission).

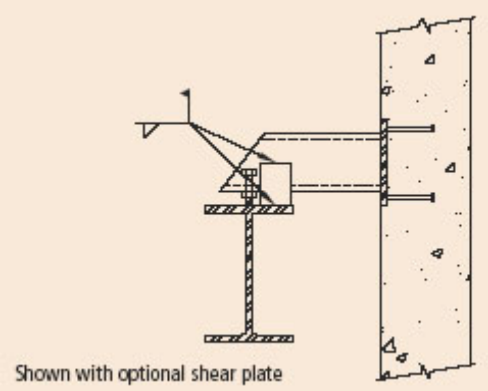

Figure 1.5 Bearing connection (from Precast/Prestressed 2007, by permission).

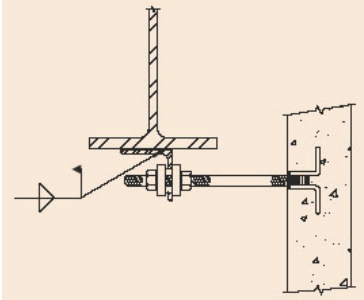

Figure 1.6 Tieback connection (from Precast/Prestressed 2007, by permission).

The connection system determines panel movement in a seismic event. For cladding wall panels as shown in Figure 1.7, the panel is rigidly fixed to and translates with the floor beam at the panel bottom. The in-plane seismic force creates shear forces at the bearing connections, where these forces and gravity loads must be resisted. Some designers prefer to provide gravity support for the panel at the top and put the tieback connections at the bottom (Fig. 1.8).

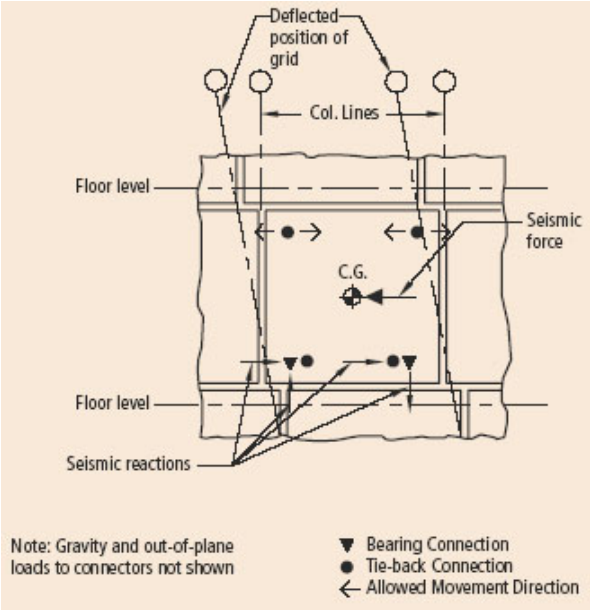

Figure 1.7 Seismic drift effect (from Precast/Prestressed 2007, by permission).

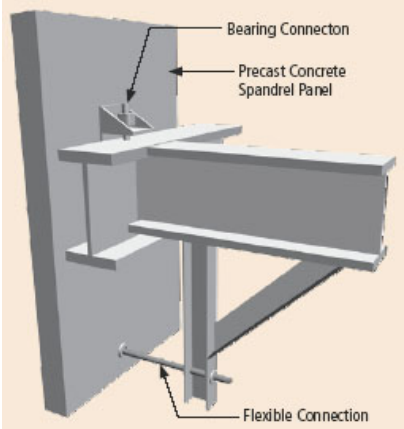

Figure 1.8 Cladding connections (from Precast/Prestressed 2007, by permission).

If the bearing connections allow lift-off, the panel may rotate ("rocking") when subjected to seismic forces (Fig. 1.9). The entire panel weight would then be carried on a single lower connection. Because the movement would occur in both directions, each bearing connection must be designed to carry the full weight of the element (Precast/Prestressed 2007).

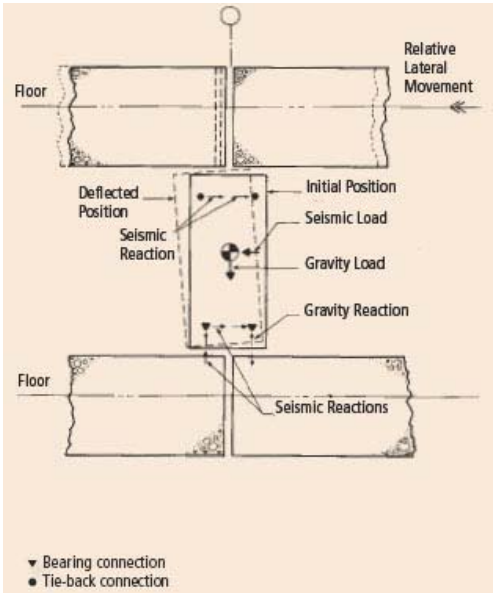

Figure 1.9 In-plane rotation (from Precast/Prestressed 2007, by permmission).

1.3 Scope of this study

This research examines the seismic energy dissipation potential of steel structures by focusing on new types of specially engineered cladding-to-frame connections. Two different mechanisms of energy dissipation were examined on a reference structure. First, the cladding connection stiffness and mass of the precast cladding were investigated as a distributed system and designed to minimize structural response when subjected to moderate seismic events, in concept similar to multiple tuned mass dampers (MTMD). Second, hysteretic energy dissipation within the connection was investigated as a means of dissipating energy during larger seismic events. This latter mechanism is closer to that studied by Pinelli et al (1995). Hysteretic behavior of individual cladding-to-frame connections was obtained through non-linear time history analysis of 3-dimensional Finite Element models using ANSYS. This behavior was then input into OPENSEES models of a reference SAC 3-story building. Analysis included time history input and non-linear response including hysteretic behavior of cladding connections.

CHAPTER 2

LITERATURE REVIEWS

2.1 Introduction

In this chapter a literature review is presented. It consists of background research on the analysis of structures that include cladding components (Section 2.2), the effectiveness of engineered cladding connections (Section 2.3), tuned mass damping systems (Section 2.4), and the reference structure used in this research (Section 2.5).

2.2 Research on cladding-structure interaction

Henry and Roll (1986) attempted to evaluate the effects of cladding systems on the lateral displacements and dynamic characteristics of a reinforced concrete moment resisting frame when the cladding was incorporated into the analysis. They developed two computer models to analyze the structure and reported that once the cladding took part in the behavior of the structure, the natural period of vibration changed significantly. This change in behavior was caused by the cladding binding up against the frame due to inadequate clearance.

Cohen and Powell (1993) studied the idea of utilizing steel cladding panels and energy-dissipating connections for seismic-resistant design. Hysteretic energy was dissipated when deformations in connections due to inter-story drift exceeded the elastic regime. The connections were hypothetical with assumed stiffness and yield strength. In their analytical study, one hypothetical steel-framed building was designed at three different levels of strength and stiffness when subjected to UBC design loads resulting in three bare frames with different member sizes. The building had five stories and three bays in one direction and five bays in the other direction. Details of the building and

design loads can be found in Cohen and Powell (1993). Three unclad frames were designed in accordance with UBC. The first frame was designed to meet strength requirements for 100 percent of the UBC loads. However it was assumed that there were deficiencies in this frame during construction and the frame was retrofitted by using structural cladding. The second frame was designed to meet the strength requirements for 25 percent of UBC loads. The third frame was designed for gravity load only. The steel cladding panels were added to these three frames to provide additional strength and stiffness to meet the UBC drift and strength requirements. Steel cladding panels were considered as very stiff plates surrounded by beams and columns to provide additional lateral stiffness to the frame. A reference frame was designed to meet 100 percent of strength and stiffness requirements of the UBC without any structural contributions from the cladding. The inelastic cladding-to-frame connections were designed to be the primary source of energy dissipation due to yielding of connections.

A two-dimensional computer model was constructed with connections modeled as zero-length elements with bilinear hysteretic behavior. Elastic stiffnesses of connections were selected based on inter-story drifts of the frame. Drift limits of the frame were used to determine yield displacements of connections. Two strain-hardening ratios for the stiffness of connections were used: 0.0 and 0.1. The analysis results showed that the fundamental periods of all three frames were altered when cladding panels and cladding-to-frame connections were included in the model. Comparing the reference frame without cladding and the three clad frames, inter-story drifts were decreased up to 42% percent and the rotations of plastic hinges in beams were reduced up to 73.8% when cladding and connections were included.

However, there were some limitations in this research. The behavior of cladding-to-frame connection was exclusively hypothetical. It was not proved that the assumed behavior of this connection is practical. Also, the attachment between the steel cladding panel and the frame in which the steel panels may provide additional stiffness to the frame was completely assumed without any practical configurations.

Palsson et al. (1984) published their results on the influence of precast concrete cladding on the dynamic response of tall buildings. In this research, the influence of precast concrete cladding on the dynamic behavior of a 25-story building was investigated. A linear elastic computer model of the steel frame was developed. Stiffness from cladding panels was considered by matching analytical frequencies from the frame analysis with values obtained from vibration tests of the real building. The bare frame and the frame with additional stiffness from cladding were then analyzed with different ground motion records. Results including peak roof displacement and inter-story drift of the clad and unclad frame were compared. Results indicated that the cladding system significantly altered dynamic characteristics of the structure leading to different seismic structural responses. The cladding system may lead to a structure which is more or less dynamically sensitive to certain earthquake ground motions leading to higher or lower structural responses. The effect of the cladding system was dependent on dynamic characteristics of the frame and the earthquake applied.

2.3 Effectiveness of engineered connections

Pinelli et al. (1990, 1992, 1993, 1995 and 1996) and Craig et al. (1992) published analytical and experimental results on utilizing cladding-to-frame connections as a source of energy dissipation. In this research connections were specifically detailed to absorb

energy during an earthquake. The horizontal shear forces due to earthquakes deform the connections. When the deformation exceeds the elastic regime, the yielding of steel is initiated. Energy dissipation within connections as a result of this inelastic response could be used to transfer demands away from the steel structure. To evaluate the potential, physical tapered tube cladding-to-frame connections with varied geometry and different types of attachment (bolted or welded) were tested (Pinelli et al. 1993). General geometry of the proposed "optimal" connection can be seen in Figure 2.1. Properties evaluated for different connection types included stiffness, ductility, energy dissipation and fatigue behavior. Testing was quasi-static. Potential energy dissipating ability of this prototype connection was demonstrated through the physical test results as shown in Figure 2.2. The actual effect of the prototype connection on the structure subjected to seismic excitations was investigated through a two-dimensional computer simulation. The analysis used properties of a real test frame constructed by National Center for Earthquake Engineering Research (NCEER) (Reinhorn et al. 1989). This frame was 1:4 scaled model representing a six-story three-bay moment resisting steel frame building. The frame was 216 in (546 cm) high and 144 in (366 cm) wide. The weight of the frame was 42 kips (19.051 kg). The unscaled periods for the two first modes were measured to be 0.85s and 0.26s.

In the computer model, the cladding connections were represented by parallel-series models made of a combination of linear springs and Coulomb slip elements as indicated in Figure 2.3 with properties based on the physical tests of connection hysteretic behavior (Craig et al. 1992). Results from the experiment and analytical model were in good agreement.

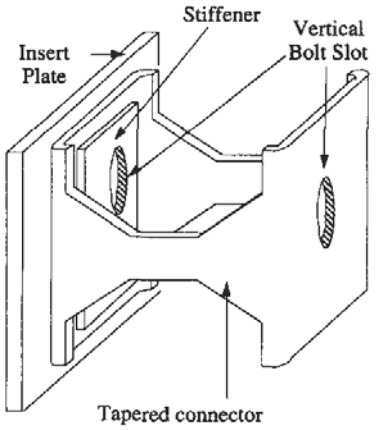

Figure 2.1 Prototype cladding connection from Georgia Tech (Pinelli et al. 1993).

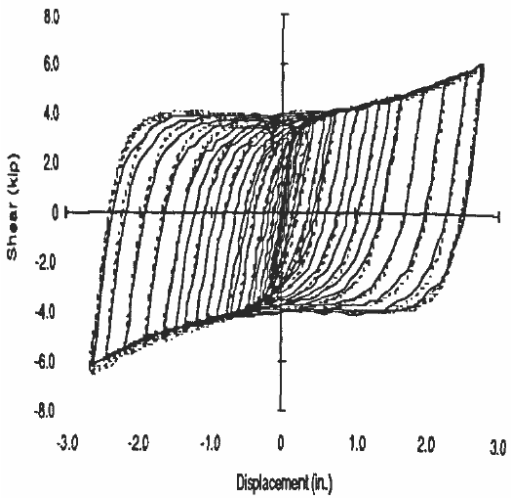

Figure 2.2 Prototype connection hysteretic behavior (Pinelli et al. 1993).

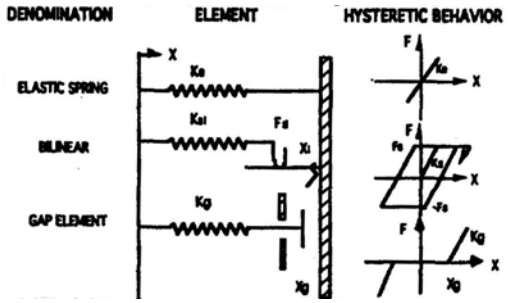

Figure 2.3 Cladding connection model (Craig et al. 1992).

During a time history loading, the seismic energy input to the overall structure (E_i) is balanced by the relative kinetic energy (E_k); the recoverable elastic strain energy (E_e); the viscous damping energy (E_d) and the irrecoverable hysteretic energy (E_h) as shown in the following equation (Uang and Bertero 1990):

$$E_i = E_k + E_e + E_d + E_h \tag{2.1}$$

In Pinelli et al. (1993), the hysteretic energy E_h consisted of hysteretic energy in structural members E_s and hysteretic energy in cladding connections E_c. To avoid yielding and damage to the structural members the researchers attempted to concentrate these in the cladding connections. Results showed that E_h was mostly dissipated by cladding connections. The effectiveness of energy dissipation of connections was measured by the ratio $\frac{E_c}{E_i}$; where E_c was the total hysteretic energy dissipated in all cladding connections.

Analysis results described in these terms are shown in Table 2.1. The "reference case" is the case of rigid connections that dissipate no energy. The ideal case is the case that the cladding panels are attached to the frame by hypothetical elastoplastic connections. The tapered case is the case that the cladding panels are attached to the frame by the prototype tapered connections. For all three earthquake records included, the frequencies of the structure were changed when the ideal or prototype connections were used. The critical finding was that all of the energy dissipation in structural members (E_s) was completely eliminated for 2 of the 3 records, with 96% reduction in the other record.

The effectiveness of the connections in dissipating energy of structures depended on the location of the fundamental frequencies of the original structures with respect to the predominant frequencies of the earthquake ground motions (the frequencies at which

the peak of the response spectrum occurs). In the case of El Centro (predominant frequency was 1.5-1.8 Hz) and Chilean (predominant frequency was 1.2-1.4 Hz) ground motions, when the ideal or prototype tapered connections were used, the fundamental frequencies of the structures increased to be in between the range of predominant frequencies. This increased the overall energy input into the structure even though all inelastic energy dissipation was still transferred to the cladding connections. For example, in the Chilean case, the total energy input to the structure increased 55%, due to the change of frequencies when ideal or prototype tapered connections were used (Fig. 2.4 a, b). On the contrary, for the Santa Barbara case, energy input to the structure was reduced by 56%, when the fundamental frequency of the original structure is higher than the predominant frequency of the earthquake (Fig. 2.4c, d). However, in all three cases story-drift was reduced (Fig 2.5a, b and c). It was seen that energy dissipating connections helped to reduce the seismic response.

Table 2.1 Case study results from Georgia Tech (Pinelli at el. 1993).

	125% El Centro			100% Chile			200% Santa Barbara		
	f (Hz)	E_s/E_i (%)	E_c/E_i (%)	f (Hz)	E_s/E_i (%)	E_c/E_i (%)	f (Hz)	E_s/E_i (%)	E_c/E_i (%)
Reference Case	1.11	37	0	1.1	34	0	1.1	32	0
Ideal Case	1.39	0	75	1.4	4	70	1.4	0	79
Tapered Case	1.35	0	74	1.4	4	70	1.3	0	64

Through the Georgia Tech research, it was shown that engineered connection design can result in significant changes to structure behavior. Not only can the fundamental frequencies of the structure be changed but inelastic action can be transferred predominantly into the cladding connections, resulting in lower story drifts throughout the structure. However, there may be some practical problems associated with

the proposed connections. The effects of proposed connections were examined in only one analytical building. Response of cladding including displacements, and expected damage in connections under earthquakes were not presented. It may be difficult to determine which connections have already yielded and should be replaced after an earthquake. Replacement of damaged connections could be an expensive and time consuming repair.

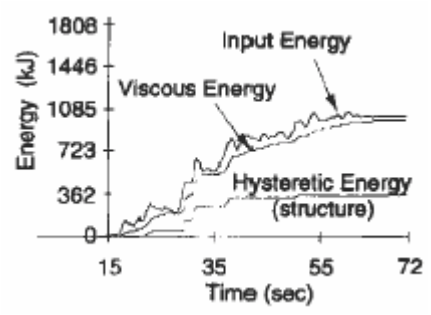

a) Energy Time history-Conventional-Chile

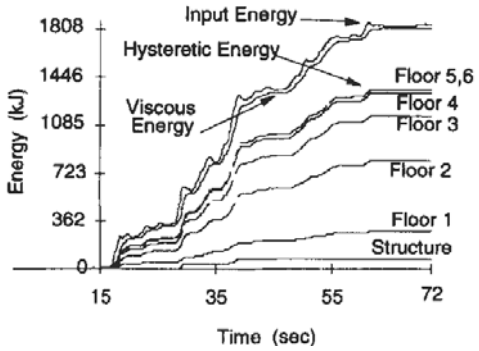

b) Energy Time History-Tapered-Chile

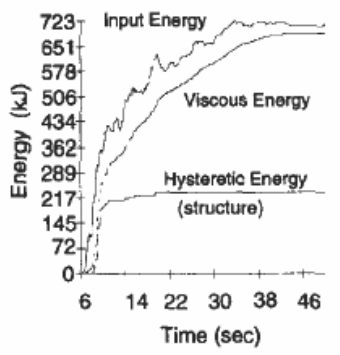

c) Energy Time history-Conventional-Santa Barbara

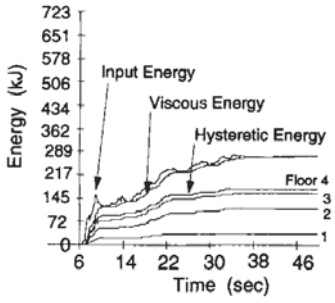

d) Energy Time History-Tapered-Santa Barbara

Figure 2.4 Energy time history results (Pinelli et al. 1995).

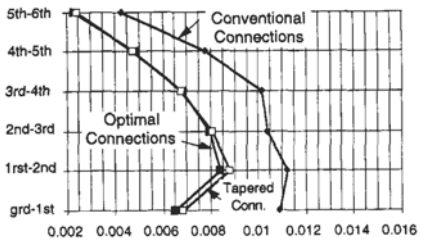

a) Drift Envelopes - El Centro

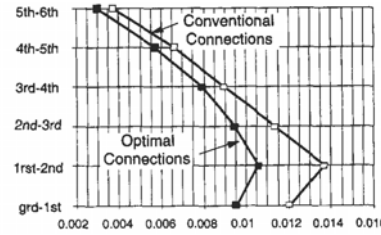

b) Drift Envelopes – Chile

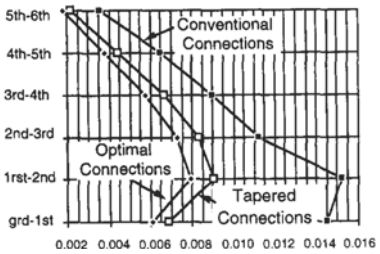

c) Drift Envelopes - Santa Barbara

Figure 2.5 Reduction in story drift when tapered tube connection were used (Pinelli et al. 1995)

2.4 Tuned mass dampers and cladding systems

From the literature review presented, cladding systems can have a significant effect on structural response, especially when engineered for this purpose. A mechanism to dissipate energy which based on the concept of tuned mass damper was evaluated in this research.

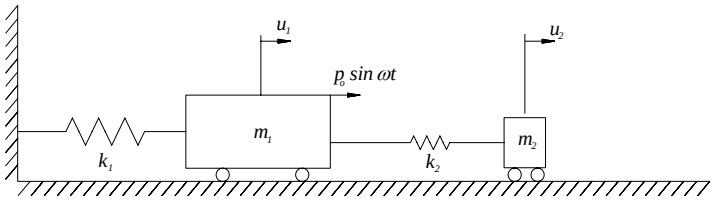

Figure 2.6 A simple model of tuned mass damper.

Consider a very simple two-degree-of-freedom system as shown in Fig 2.6. The first mass m_1 is roughly assumed to represent the mass of the structural frame. A cladding panel has its own mass (m_2) and is shown connected to the frame by a connection which has a specific stiffness k_2. This cladding panel and its connector system are similar to a tuned mass damper consisting of a spring k_2 and a mass m_2. When a harmonic force $p = p_o \sin \omega t$ is applied, equations of motion for this two degree-of-freedom system that can be found in many dynamics textbooks are as follows:

$$\begin{bmatrix} m_1 & 0 \\ 0 & m_2 \end{bmatrix} \begin{Bmatrix} \ddot{u}_1 \\ \ddot{u}_2 \end{Bmatrix} + \begin{bmatrix} k_1 + k_2 & -k_2 \\ -k_2 & k_2 \end{bmatrix} \begin{Bmatrix} u_1 \\ u_2 \end{Bmatrix} = \begin{Bmatrix} p_o \\ 0 \end{Bmatrix} \sin \omega t \tag{2.2}$$

The solution for this system of equations is

$$\begin{Bmatrix} u_1(t) \\ u_2(t) \end{Bmatrix} = \begin{Bmatrix} u_{1o} \\ u_{2o} \end{Bmatrix} \sin \omega t \tag{2.3}$$

in which:

$$u_{1o} = \frac{p_o}{k_1} \frac{1 - \left(\frac{\omega}{\omega_2^*}\right)^2}{\left[1 + \mu\left(\frac{\omega_2^*}{\omega_1^*}\right)^2 - \left(\frac{\omega}{\omega_1^*}\right)^2\right]\left[1 - \left(\frac{\omega}{\omega_2^*}\right)^2\right] - \mu\left(\frac{\omega_2^*}{\omega_1^*}\right)^2} \tag{2.4a}$$

$$u_{2o} = \frac{p_o}{k_1} \frac{1}{\left[1 + \mu\left(\frac{\omega_2^*}{\omega_1^*}\right)^2 - \left(\frac{\omega}{\omega_1^*}\right)^2\right]\left[1 - \left(\frac{\omega}{\omega_2^*}\right)^2\right] - \mu\left(\frac{\omega_2^*}{\omega_1^*}\right)^2} \tag{2.4b}$$

$$\omega_1^* = \sqrt{\frac{k_1}{m_1}} \quad \omega_2^* = \sqrt{\frac{k_2}{m_2}} \quad \mu = \frac{m_2}{m_1} \tag{2.5}$$

From Equation 2.4a, u_{1o} vanishes when $\omega_2^* = \omega$. It is seen that a properly tuned mass damper can reduce the response amplitude of the system subjected to sinusoidal load to near zero. The concept remains valid when applying for more complicated systems with a large number of degrees-of-freedom. In practice, tuned mass dampers have been widely used for buildings subjected to wind induced vibrations.

For this research the cladding systems are defined as two components: the heavy precast concrete panels and connections between cladding panels and the structural frame. The concrete panels are divided into individual units defined by the floor-to-floor height, and the bay width. Joints are provided between panels so that panels do not collide with one another during seismic events. If we consider each cladding panel as an individual oscillator attached to the frame through connections (Fig. 2.7), we have a structure which could be adapted into a multiple tuned mass damper system. It has been shown that the effectiveness of MTMD depends on the range of natural periods of the distributed oscillators (Xu & Igusa 1992, Abe & Fujino 1994). Energy dissipation is more effective when natural periods of MTMD are closely distributed around the natural period of the main structure (Igusa & Xu 1994). For cladding systems, the weights of cladding panels are usually governed by architectural factors and may not be largely varied. However, the stiffness of the cladding-to-frame connections can be varied through design, thereby modifying the natural periods of the MTMD. By engaging the cladding systems distributed throughout a structure as MTMD the response of the building under earthquakes may be modified.

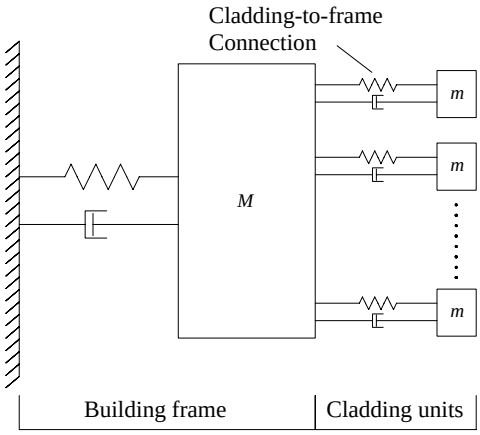

Figure 2.7 Cladding system as an elastic distributed damping system.

2.5 Reference structures

The frame to be investigated in this study is a moment-resisting frame used in the SAC project, co-developed by three organizations: The Structure Engineers Association of California (SEAOC), The Applied Technology Council (ATC) and California Universities for Research in Earthquake Engineering (CUREE). The SAC structures have been widely used in research on control problems of buildings under seismic excitations. Three different SAC structures were developed, a 3-story building, 9-story building and 20-story building. The first natural periods of these structures are reported to be 1.01s, 2.27s and 3.84s respectively (Ohtori et al. 2004). The SAC 3-story building was selected as the reference structure in this research to calibrate analysis results with other research that has been carried out and contribute new results to related research. This smaller structure was selected for initial research to simplify the models. Future research could apply results to the 9 and 20 story buildings. The building is 3-floor 4-bay moment resisting steel frame. Specifics of the structure are modeled after Ohtori et al. (2004). The frame geometry can be seen in Figure 2.8.

Figure 2.8 3-story SAC building.

CHAPTER 3

CLADDING AS AN ELASTIC DISTRIBUTED DAMPING SYSTEM

3.1 Introduction

This chapter investigates the concept of utilizing cladding as an elastic distributed damping system. A computer model was developed in SAP2000 to initially investigate this potential. Since the MTMD was initially envisioned as a means to prevent yielding of structural members as well as cladding connections under moderate seismic loading this initial investigation only considered elastic material properties. Results were then investigated for non-linear material behavior as discussed in Chapters 4 and 5.

3.2 Analysis model

To evaluate the potential to utilize cladding system as MTMD, the reference structure was modeled in SAP2000 with cladding panels included. The structure was modeled as a 2D frame with all out-of-plane degrees-of-freedom restrained. Frame elements were assigned steel material with linear elastic behavior. The elastic modulus of steel was 29,000 ksi (199,947 Mpa). Member offset lengths were automatically calculated by SAP2000. Seismic masses of the frame consisted of the steel framing, floor slabs, ceiling/flooring, mechanical/electrical, partitions, roofing and a penthouse located on the roof and were taken as defined in Ohtori et al. (2004). Seismic masses were lumped at frame joints. Seismic mass at each joint of the first and second levels was 6.55 kip-s^2/ft (9.57 x 10^4 kg) and the third level was 7.10 kip-s^2/ft (1.04 x 10^5 kg) (Fig. 3.1a). The structure details were as note in Ohtori et al. (2004).

From this basic SAC frame, the connections between cladding panels and the frame were added as elastic frame elements with the length of 1 foot (0.3 m). The

cladding panels were modeled as lumped sum masses at the cladding end of each connection. Cladding masses were calculated as the sum of mass of quarters of surrounding panels (Fig. 3.2). The panels were assumed to have 6 in (0.15 m) thickness of concrete with weight density of 145 lb/ft^3 (2323 kg/m^3). Mass of cladding panel at a joint surrounded by 4 quarters of cladding panel was calculated as (0.145kip/ft^3)(0.5ft)(13ft)(30ft)/(32.2ft/sec^2) = 0.88 kip-sec^2/ft (1.29 x 10^4 kg). To account for other components of the wall assemblies, a mass value of 1 kip-sec^2/ft (1.46 x 10^4 kg) was used.

The boundary conditions at base of columns were fixed. At each frame joints, only movements in the plane of the frame were allowed. Rotations at ends of cladding elements were allowed.

The structure was first analyzed with no cladding masses to calibrate results with Ohtori et al. (2004) and then analyzed with masses and varying lateral stiffness in the cladding connections included. One-hundred modes of vibration were considered in the dynamic analysis. This guaranteed sufficient modes of vibration were considered with the sum of modal participations was almost 100%. The lateral stiffness was varied by changing the connection thickness, while maintaining all other dimensions and properties constant. The weightless connection cross section was arbitrarily assumed to be rectangular with a height of 1 foot (0.15 m) and varying width from 0.018 ft (0.005 m) to very large (approaching rigid) values. It is important to note that any connection with a similar lateral stiffness would provide similar results, so at this stage a simple rectangular section was adopted.

Natural vibration period of the connection itself was calculated as a cantilever beam with one end fixed and the other end located a lump sum mass representing the cladding panel (Fig. 3.1). As noted previously, the connection boundary conditions were simplified at this stage of analysis. Actual conditions would be dependent on the cladding to connection detailing. Similar stiffness could be obtained with different boundary conditions combined with other lengths or cross sectional properties.

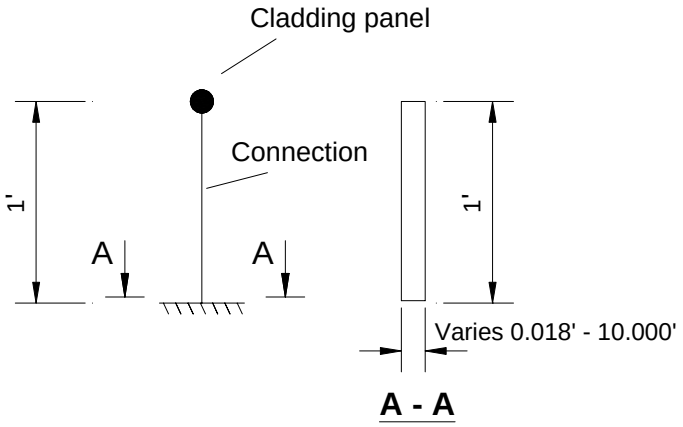

Figure 3.1 Calculation model for natural vibration of connection.

3.3 Analysis results and discussion

Without cladding masses, the first three periods of the structure were found to be 0.97s, 0.32s and 0.17s. These results agree with the analysis results by Ohtori et al. (2004) (1.01s, 0.33s and 0.17s respectively). Variations are likely due to slightly different structure details used such as the length of member offset, material properties and the conversion of unit systems. These details were not available in Ohtori et al. (2004).

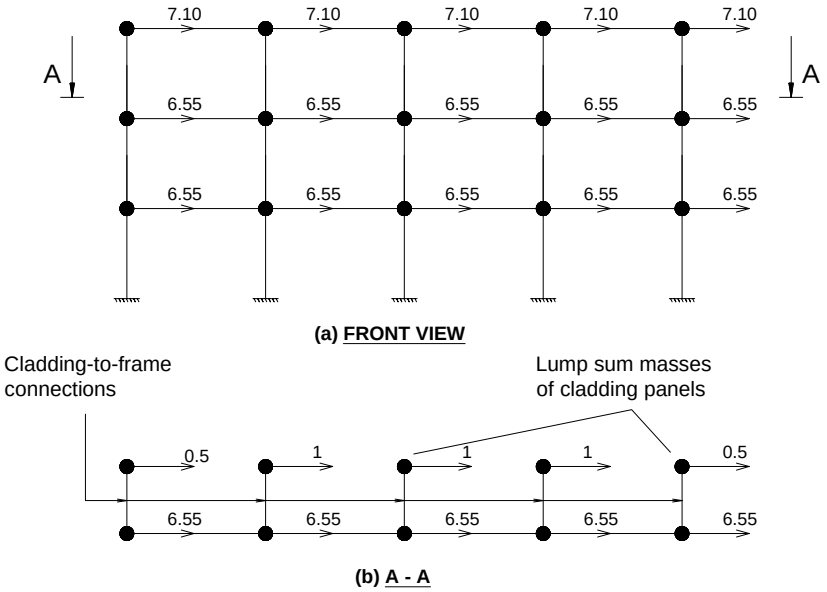

Figure 3.2 Lump sum masses locations.

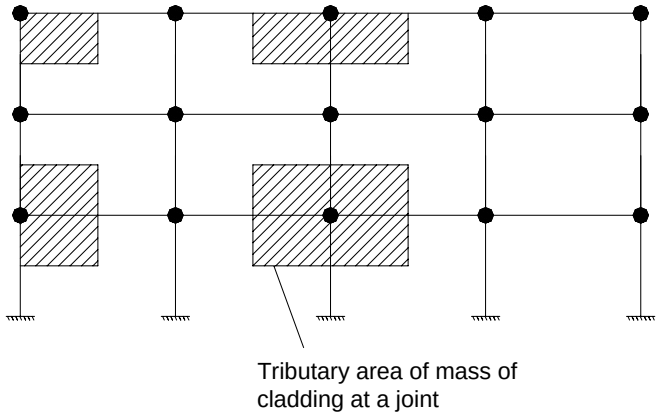

Figure 3.3 Tributary areas of cladding masses at different locations.

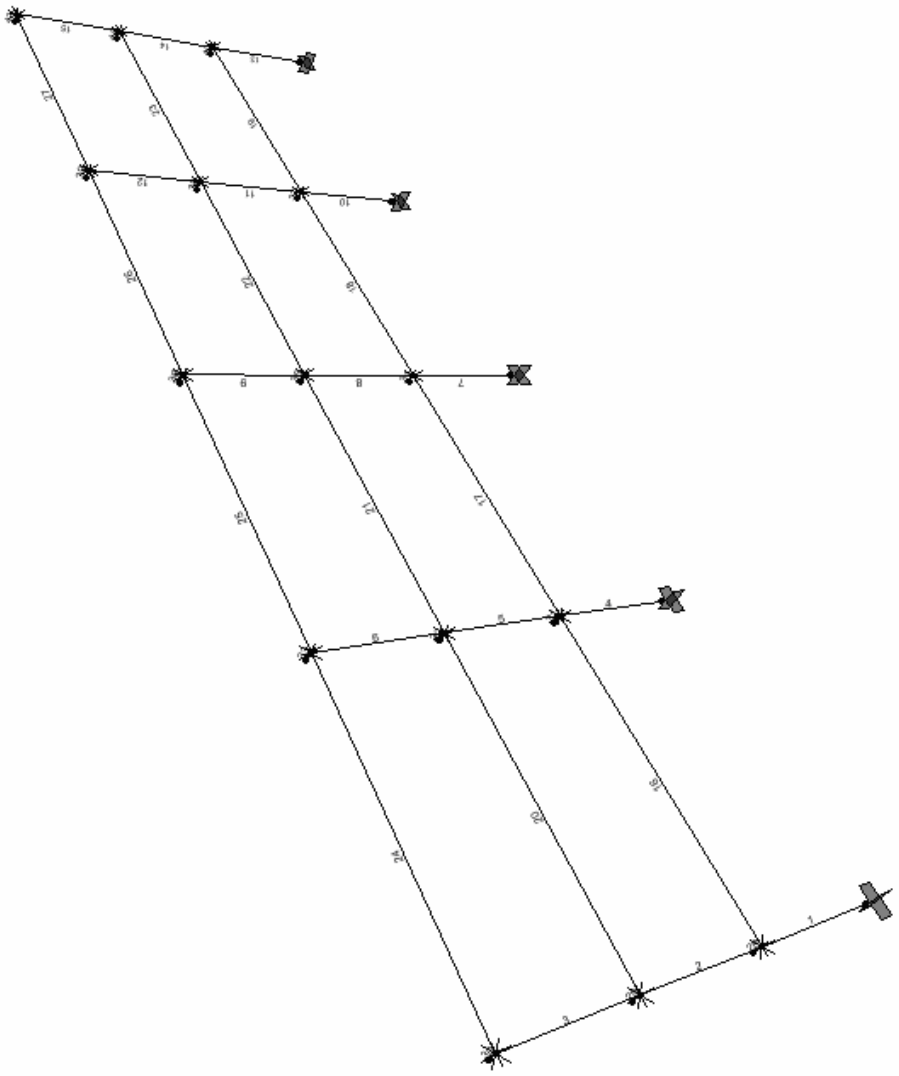

Figure 3.4 SAP2000 model.

Mode 1 (0.97s) Mode 2 (0.32s) Mode 3 (0.17s)

Figure 3.5 Mode shapes of the three-story model.

Table 3.1 presents the dynamic analysis results of the structure as the lateral stiffness of the cladding-to-frame connections was varied. The free vibration of the structure changed when the cladding panels were introduced. When the lateral stiffness of the connections was 1.04E+03 kip/ft (15.2E+03 kN/m) or larger, free vibration of the structure was not affected. When the stiffness of the connections varied from 1.04E+03 kip/ft (15.2E+03 kN/m) to 1.04E+09 (15.2E+09 kN/m) kip/ft, the first three periods did not vary more than 1%. The mass participation ratios also mostly remained similar.

Table 3.1 Three-story dynamic analysis results.

Connection stiffness (kip/ft)	Natural Period of Cladding Units (s)	1st Period (s)	Participation Ratio	2nd Period (s)	Participation Ratio	3rd Period (s)	Participation Ratio	Sum of participation of first three modes	Δ^* (%)
No cladding	-	0.97	0.84	0.32	0.13	0.17	0.02	0.990	-
1.04E+09	0.000	1.01	0.82	0.33	0.12	0.18	0.02	0.967	99.98
1.31E+08	0.001	1.01	0.82	0.33	0.12	0.18	0.02	0.969	99.95
1.04E+06	0.006	1.01	0.82	0.33	0.12	0.18	0.02	0.970	99.39
1.31E+05	0.017	1.01	0.82	0.33	0.12	0.18	0.02	0.970	98.27
1.63E+04	0.049	1.01	0.82	0.33	0.12	0.18	0.02	0.970	95.11
1.04E+03	0.194	1.01	0.82	0.34	0.12	0.17	0.01	0.957	80.68
130.50	0.550	1.01	0.82	0.31	0.09	0.17	0.02	0.937	45.78
66.82	0.769	1.03	0.81	0.31	0.11	0.17	0.02	0.934	25.37
57.29	0.830	1.04	0.79	0.31	0.11	0.17	0.02	0.915	20.07
44.76	0.939	1.07	0.68	0.32	0.11	0.17	0.02	0.815	11.86
34.21	1.074	1.14	0.41	0.96	0.37	0.32	0.11	0.895	5.50
28.19	1.183	1.22	0.25	1.00	0.48	0.32	0.11	0.845	18.66
22.92	1.312	1.34	0.16	1.04	0.45	0.32	0.11	0.723	26.74
16.31	1.556	1.57	0.10	0.93	0.51	0.32	0.11	0.722	66.89

Connection stiffness (kip/ft)	Natural Period of Cladding Units (s)	1st Period (s)	Participation Ratio	2nd Period (s)	Participation Ratio	3rd Period (s)	Participation Ratio	Sum of participation of first three modes	Δ* (%)
11.12	1.884	1.90	0.08	0.98	0.39	0.32	0.11	0.580	92.16
8.35	2.174	2.18	0.07	0.95	0.66	0.32	0.11	0.843	128.12
6.09	2.546	2.56	0.06	0.96	0.72	0.32	0.11	0.891	164.65

* Δ = Difference between period of the highest participation and natural period of cladding units.

If the lateral stiffness of the connection was low enough (less than 34.21 kip/ft (499.2 kN/m), it is seen that the structural dynamic properties were significantly different. When the stiffness of the connection reduced from rigid to 22.92 kip/ft (334.5 kN/m), the first period lengthened 30%, increasing from 1.01s to 1.34s. The mass participation of the first mode of vibration changed significantly, reducing from 82% to 16%. The second and the third modes were also affected when the connection stiffness was varied in this range.

When the connection stiffness varied from 22.92 kip/ft (334.5 kN/m) to 6.09 kip/ft (88.9 kN/m), the first period of the structure was very close to the natural period of the cladding/connection system. The mass participation of the first mode in this range also reduced significantly. The vibration of the first mode appeared to represent the vibration component of the cladding system rather than the structural frame. In other words, a new period was introduced that was similar to the cladding period. The fundamental period of the frame was represented by the second mode with mass participation in this mode larger than other modes.

The dynamic behavior of the structure under seismic excitation was then investigated. The structure was analyzed with the El Centro earthquake ground motion acceleration (North-sourth component recorded on May 18, 1940) with PGA of 0.35g

(Fig. 3.6 and 3.7), the IBC 2000 design response spectrum (Fig. 3.8) and the BOCA 1996 design response spectrum (Fig. 3.9). Parameters of design response spectra were selected so that results from response spectrum analysis were comparable with results from time history analysis. S_{ds} of design response spectra was selected as 1g based on maximum spectral acceleration of El Centro earthquake ground motion of 0.91g. The purpose of the seismic analysis was to determine the effect of the connection lateral stiffness on the structure response. The response modification coefficient used was R = 1, and the deflection amplification factor was C_d = 1, to gain a reference value for elastic response. These analyses were performed as a general investigation only. Resulting maximum base reactions and maximum moments in the structural members for each earthquake excitation can be seen in Table 3.2. An example of maximum moment diagram due to seismic excitation is shown in Figure 3.10.

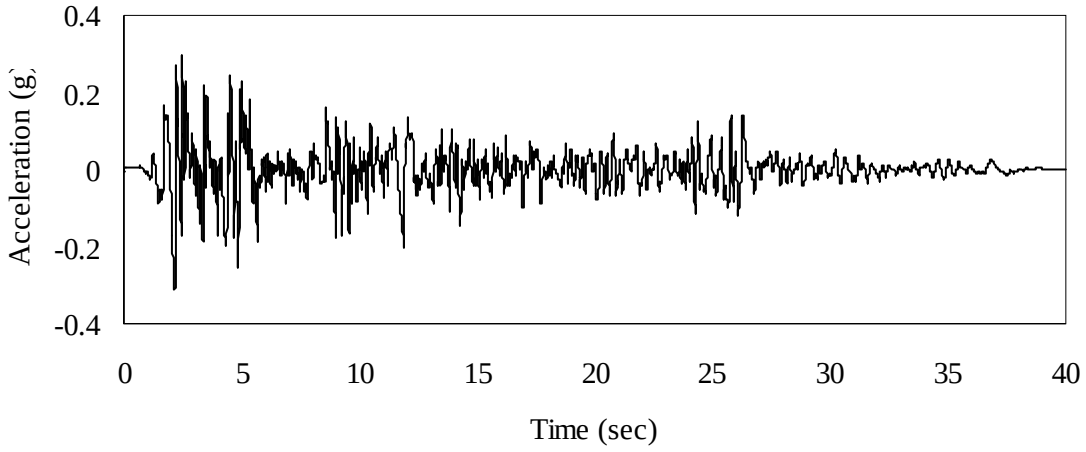

Figure 3.6 El Centro earthquake ground acceleration.

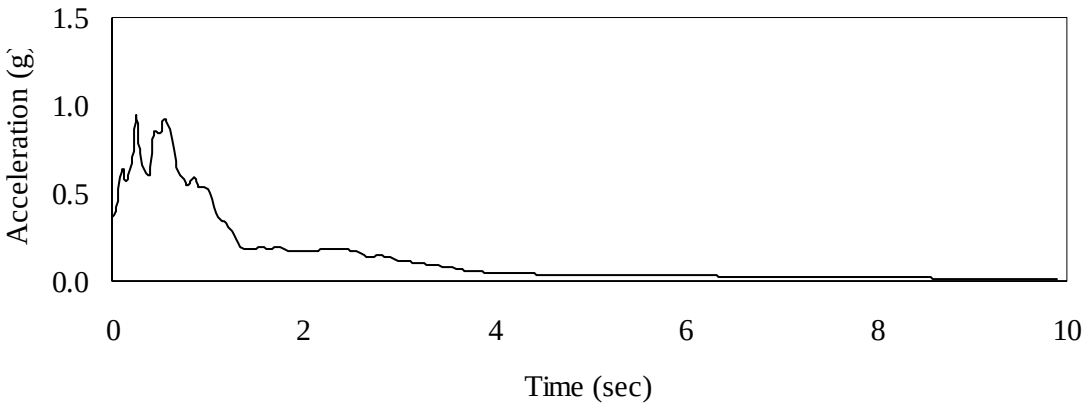

Figure 3.7 El Centro earthquake pseudo acceleration response spectra.

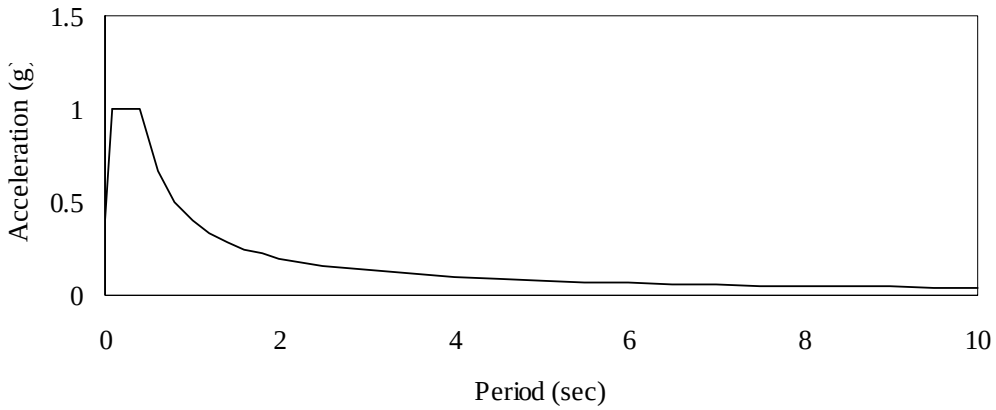

Figure 3.8 IBC2000 response spectra.

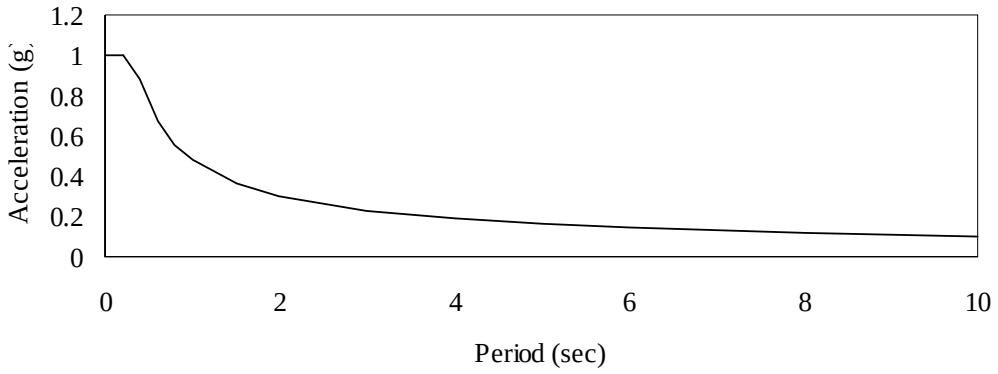

Figure 3.9 BOCA96 response spectra.

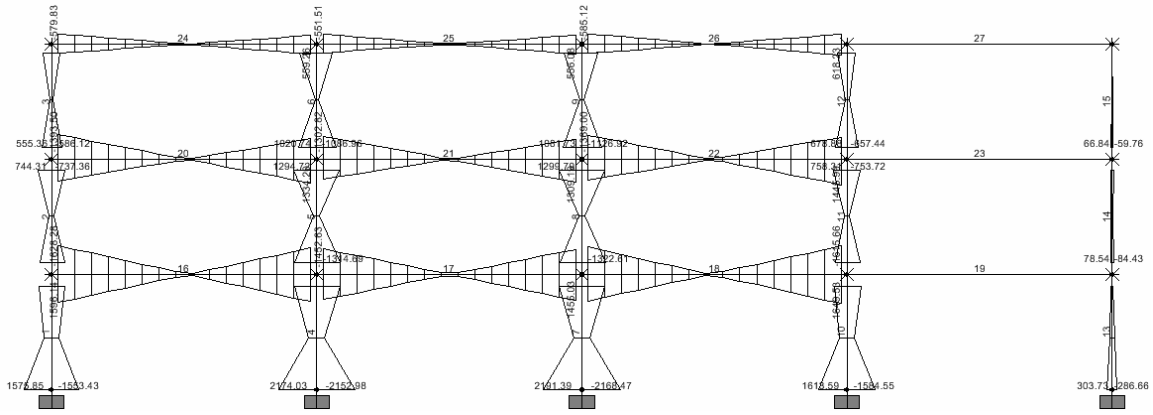

Figure 3.10 Maximum moment diagram due to El Centro Earthquake.

Table 3.2 Three-story seismic response

Connection stiffness (kip/ft)	El Centro		IBC 2000		BOCA96	
	Base Reaction (Kip)	Moment Max (Kip-ft)	Base Reaction (Kip)	Moment Max (Kip-ft)	Base Reaction (Kip)	Moment Max (Kip-ft)
66.82	1555.74	2546.29	1226.03	2086.48	1452.86	2518.85
57.29	1455.34	2379.86	1199.39	2028.81	1422.40	2454.57
44.76	1267.24	2014.12	1106.87	1842.32	1311.70	2236.20
34.21	1171.53	1860.44	992.73	1632.98	1164.14	1970.85
28.19	1088.18	1720.53	970.70	1602.13	1131.07	1923.97
22.92	1046.75	1649.53	953.71	1570.28	1102.34	1873.24
16.31	1180.06	1831.32	1005.41	1671.07	1150.75	1965.96
11.12	1390.16	2205.00	1060.93	1779.10	1215.54	2089.67
8.35	1499.03	2394.49	1137.15	1924.54	1306.10	2258.77
6.09	1566.36	2514.78	1183.08	2013.33	1363.88	2368.32

Results are plotted in Figure 3.11 and 3.12 in the range of the connection stiffness of 6.09 kip/ft (88.9 kN/m) to 66.82 kip/ft (975.1 kN/m). For all three seismic excitations, the base reaction and the maximum moment reduce to the minimum values when the stiffness of the connection was 22.92 kip/ft (334.5 kN/m). It is important to note that structural response was reduced the most when the stiffness of cladding-to-frame connections in a range where period of cladding units was similar to the fundamental period of the structural frame. Base shear and maximum moments in critical structural elements were reduced as much as 40% and 28% respectively. Dissipation of energy by the cladding system was most effective when natural periods of cladding units were similar to the fundamental period of the frame (Fig. 3.11 and 3.12).

In order to obtain 40% reduction in base shear and 28% reduction in maximum moment, the long connections were subjected to maximum relative cladding displacements to the frame of 14.6 in (0.37 m) and 13.2 in (0.34 m) respectively. These are not likely to be practical values, so means of reducing deflections were investigated. Reducing the length of the connections while maintaining the same connection overall stiffness was not an effective control of displacements. The length of connections was reduced to 6 in (0.15 m) while maintaining a stiffness of 33.41 kip/ft (487.6 kN/m). The maximum relative displacement between cladding and the structural frame decreased from 14.6 in (0.37 m) to 12.24 in (0.31 m) with approximately the same amount of base shear reduction. Smaller effective connection lengths could be achieved within a longer connection by providing a weakened zone in an otherwise stiff connection. This would be required to maintain clearance for insulation and other construction requirements. Alternatively, by adding more mass to cladding panels, stiffer connections could be used

to obtain a similar cladding-connection system fundamental period. As was noted previously, cladding weight is not likely to have a large amount of variation. However, additional mass could be incorporated by including a section of floor near the edge of the structure in the precast element. In one case with cladding masses doubled by assuming the inclusion of a portion of the floor masses, a 24% of reduction in base shear was obtained with relative maximum cladding displacement of 6.3 in (0.16 m). While a significant reduction in relative displacement was realized, this is still quite large and may not be practical. However, it was shown that there is the potential to mitigate deflections through the assumption of different design scheme while still reducing forces on the structural members.

Bending stresses in connections due to self weight of cladding panels and due to seismic force were calculated. In case of the connection which had stiffness of 22.92 kip/ft (334.5 kN/m), maximum bending stress due to self weight was 47.9 ksi (330.3 Mpa). Bending stress due to seismic force in lateral direction was 188.9 ksi (1302.4 Mpa) (Table 3.3). Stresses were high with these simplistic connections.

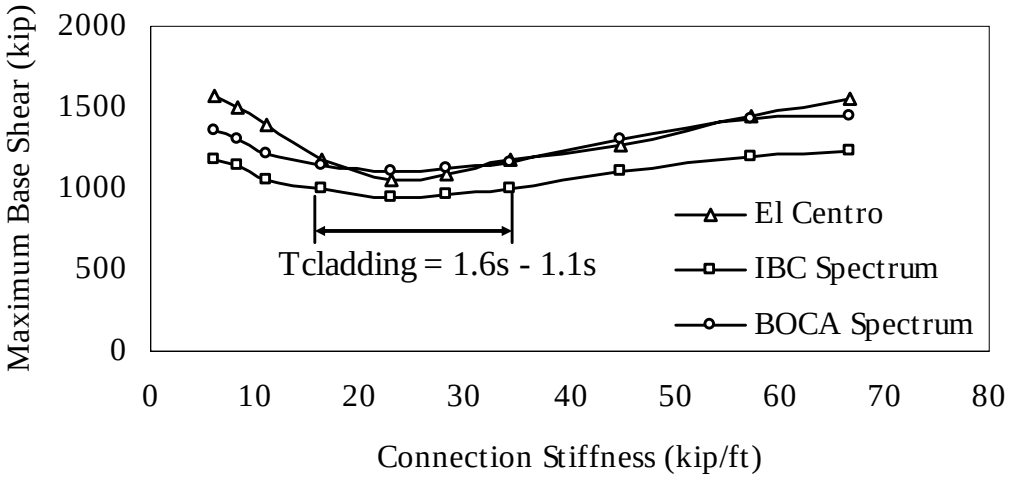

Figure 3.11 Three-story maximum base shear versus different connection stifness

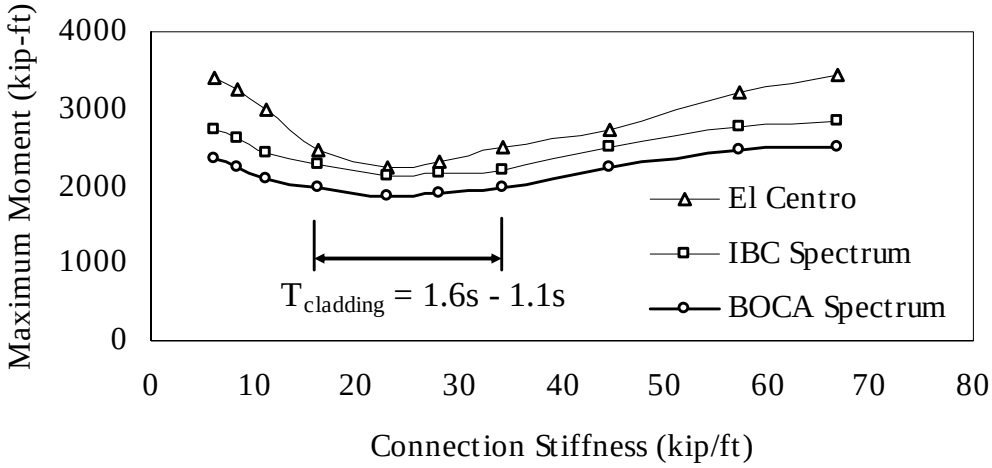

Figure 3.12 Three-story maximum moment in beams versus different connection stiffness.

Table 3.3 Bending stresses in connections.

Connection stiffness (kip/ft)	Bending stress due to self weight (ksi)	Bending stress due to seismic force (ksi)
1.04E+09	0.13	0.00
1.31E+08	0.27	0.00
1.04E+06	1.34	0.08
1.31E+05	2.68	0.32
1.63E+04	5.37	1.30
1.04E+03	13.42	10.27
130.50	26.83	31.64
66.82	33.54	72.57
57.29	35.31	108.15
44.76	38.33	157.47
34.21	41.93	157.08
28.19	44.72	127.46
22.92	47.92	188.92
16.31	53.67	176.87
11.12	60.98	207.93
8.35	67.08	180.69
6.09	74.54	99.25

3.4 Conclusion

The potential to utilize cladding systems as an elastic distributed damping system was shown, although displacements and also stresses were not controlled with the simplistic connection evaluated. Base shear was reduced as much as 40 percent and demands on structural elements were reduced as much as 28%. It is seen that cladding systems may have positive contributions to the behavior of structures when subjected to earthquake loads. Further research is necessary to control deflection and strength of connections used for energy dissipating purposes.

CHAPTER 4

HYSTERETIC ENERGY DISSIPATION CONNECTIONS

4.1 Introduction

Hysteretic energy dissipation within cladding-to-frame connections was studied as an additional means to utilize the cladding system as a source of seismic energy dissipation. During large seismic events, inelastic deformations of connections result in dissipation of energy through hysteretic damping. Promising results were reported in previous research (see Chapter 2: Literature reviews). Craig et. al. (1992) and Pinelli et al. (1993, 1995) reported the potential to utilize hysteretic energy dissipation within cladding-to-frame connections during earthquakes. Proposed energy dissipating connections were tested to evaluate several properties including stiffness, ductility, energy dissipation and fatigue behavior (Craig et al. 1992). Hysteretic behavior of the proposed connections was then incorporated into a computer model of structure. Proposed connections were reported to significantly reduce seismic responses of the structure (Pinelli et al. 1995). However, the effects of proposed connections were examined in only one analytical building. Response of cladding including displacements, and expected damage in connections subjected to earthquake load were not presented.

The use of hysteretic energy dissipation in cladding connections is also a focus of this research. To obtain hysteretic behavior of connections, non-linear time history analysis of 3-dimensional Finite Element (FEM) models of connections was performed using ANSYS. The resulting hysteretic responses were then input into structural models in OPENSEES of the SAC frame structure previously described. The objective of this

research was to define a methodology for evaluating connection performance and highlight potential benefits and areas needing further study.

Three types of connections were modeled in ANSYS: the tapered tube connection previously studied by Pinelli et al. (1993) (Fig. 4.1), the plate connection used in the elastic modeling of Chapter 3 (Fig. 4.2) and the simple composite connection (Fig. 4.3). The tapered tube connection which was based on Pinelli et al. (1993) was used for calibration of results to a complex geometry connection. The plate connection which had the same dimensions as the connection resulting in the most structural response reduction in Chapter 3 was analyzed for post yielding comparison purposes. A simple composite connection was modeled to initially investigate the potential to use composite material to develop hysteretic energy dissipation connections which result in desired hysteretic behavior.

4.2 Finite element modeling of the hysteretic energy dissipation connection

Finite element meshing of the tapered tube connection can be seen in Figure 4.4. To correctly represent the geometry complexity of the model, 3-D tetrahedral solid elements (SOLID187) were used. This element is suitable for structures with irregular geometry. This element is defined by 10 nodes with 3 degrees-of-freedom at each node. This element has the capability of taking into account plasticity, hyper-elasticity, creep, stress stiffening, large deflection and large strain effects (ANSYS 11.0 help documentation). The tapered tube connection was modeled by 1828 elements which were defined by 4117 nodes.

Finite element meshing of the plate connection can be seen in Figure 4.6. The plate connection was modeled by 3-D shell elements (SHELL181). Each element is

defined by 4 nodes with six degrees-of-freedom at each node (Fig. 4.7). This element is suitable for thin to moderately thick shell-shape structures. This element is appropriate for non-linear, large rotation and large deformation analysis (ANSYS 11.0 help documentation). The plate connection was modeled by 906 elements defined by 992 nodes.

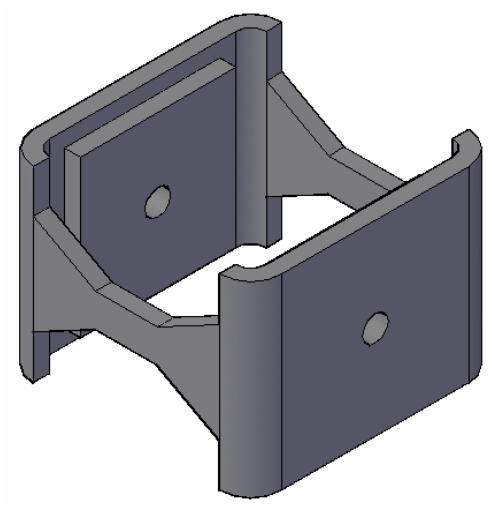

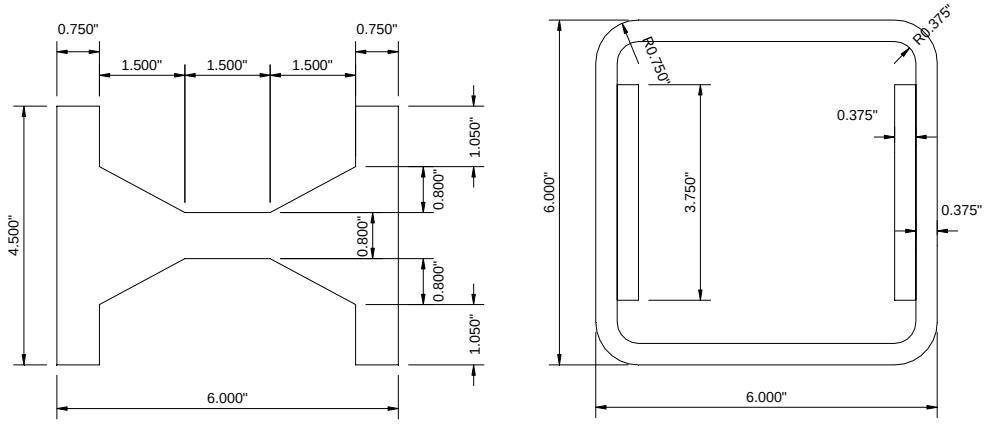

Figure 4.1 Tapered tube connection (after Pinelli et al. 1993).

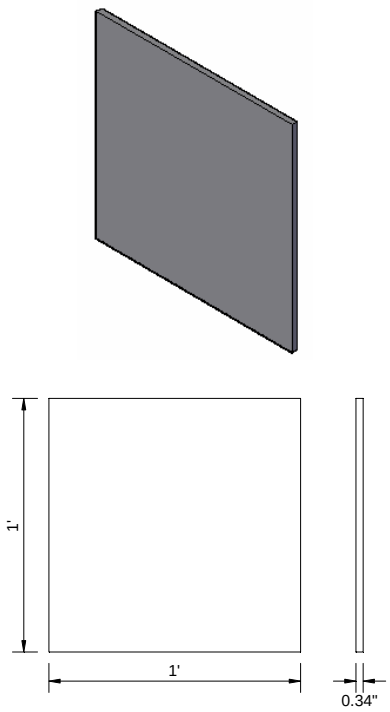

Figure 4.2 Plate connection.

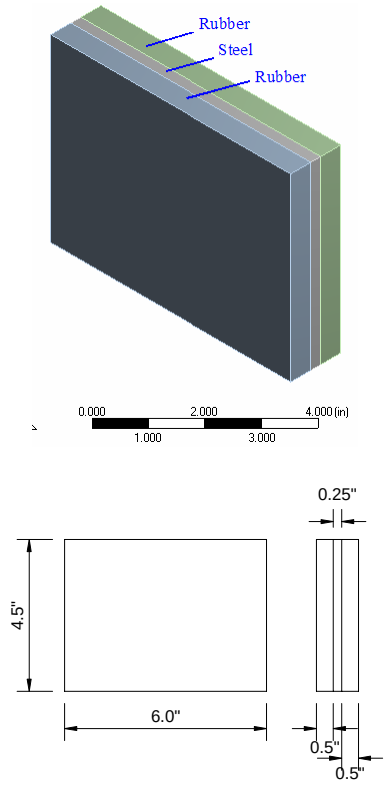

Figure 4.3 Simple composite connection.

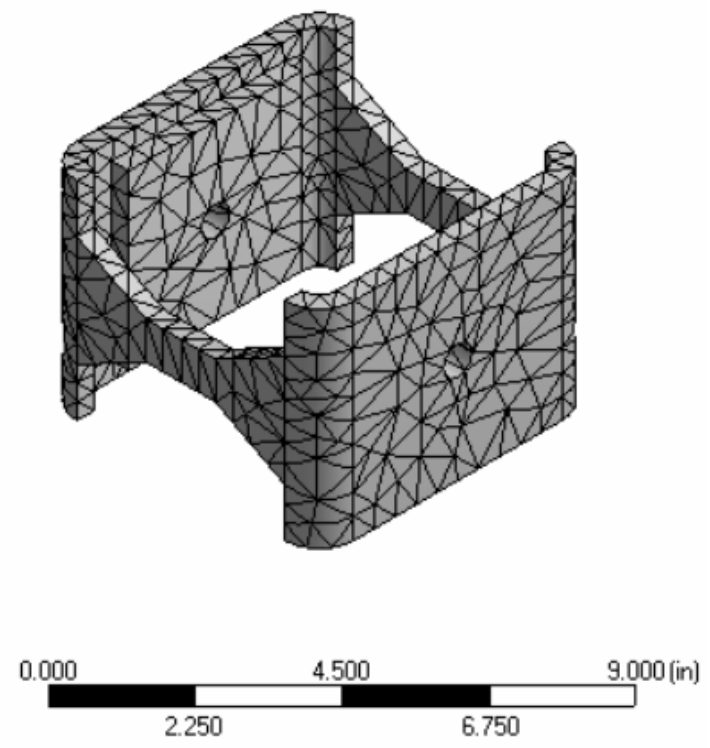

Figure 4.4 Finite element meshing of the tapered tube connection.

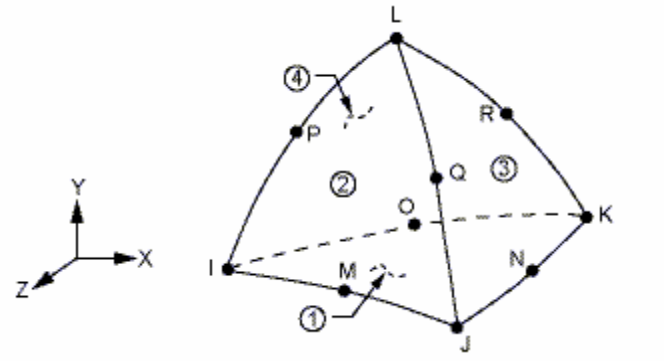

Figure 4.5 3-D finite elements for tapered tube connection (from ANSYS).

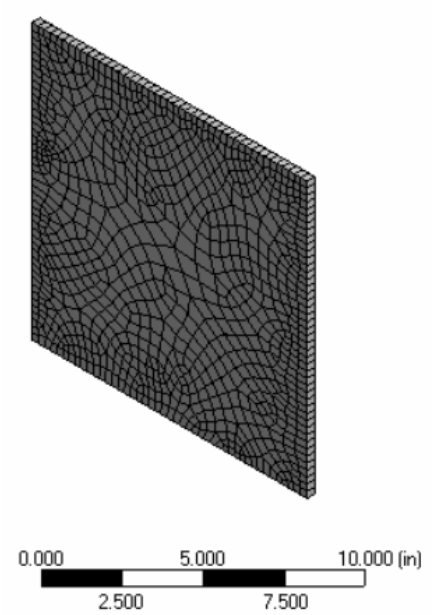

Figure 4.6 Finite element meshing of the plate connection.

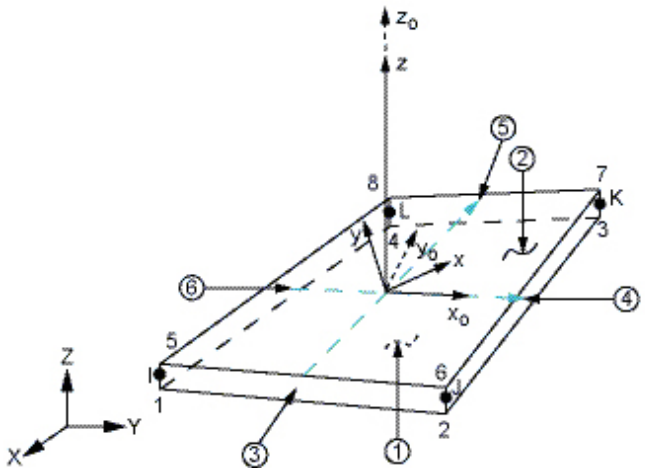

Figure 4.7 3-D finite elements for plate connection (from ANSYS).

Finite element meshing of the simple composite connection can be seen in Figure 4.8. The simple composite connection was modeled by 3-D 20-node solid elements (SOLID186). This element is defined by 20 nodes with 3 degrees-of-freedom at each node (Fig. 4.9). This element has capability of taking into account plasticity, hyper-

elasticity, creep, stress stiffening, large deflection and large strain effects (ANSYS 11.0 help documentation). This element is also able to simulate deformations of nearly incompressible elastoplastic materials and fully incompressible hyperelastic materials which was necessary to model the two outer layers of rubber. Contact regions between different material layers were modeled by 3-D surface-to-surface contact elements (CONTA174) (Fig. 4.10). This element is suitable to model contact and sliding behavior between 3-D surfaces. For preliminary modeling it was assumed that the materials could be fully bonded to each other, so this would be appropriate. Further modeling could be performed to evaluate partial bond conditions. These contact elements have the same geometric characteristics as the solid element face which they are connected (ANSYS 11.0 help documentation). The contact elements were assigned frictionless properties. The simple composite connection was modeled by 960 3-D 20-node solid elements and 1536 3-D surface-to-surface contact elements.

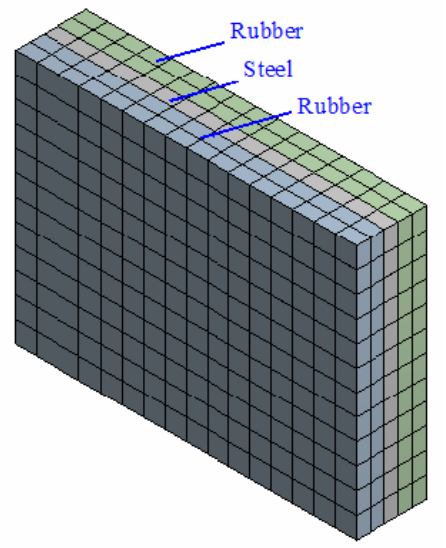

Figure 4.8 Finite element meshing of simple composite connection.

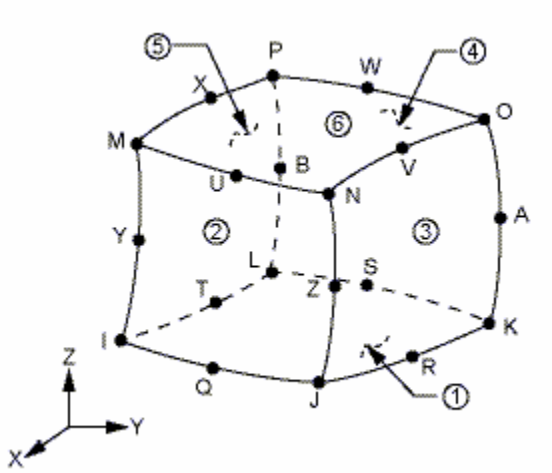

Figure 4.9 3-D finite element of simple composite connection.

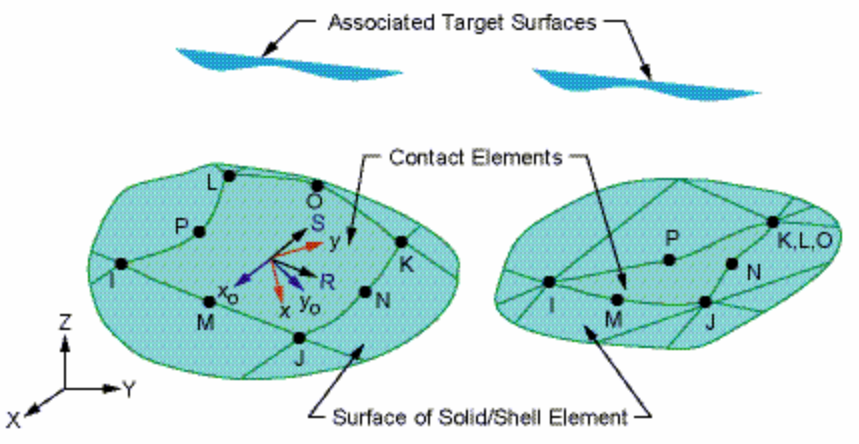

Figure 4.10 3-D contact element for simple composite connection (from ANSYS).

Bilinear kinematic hardening constitutive model was used for the steel material (Fig. 4.11). Yield stress of steel was 46 ksi (317.2 Mpa). Ultimate stress of steel was 75 ksi (517.1 Mpa). Young's modulus of steel was 29,000 ksi (199,947.6 Mpa). Tangent modulus was 29 ksi (199.5 Mpa). Poisson's ratio of steel was 0.3. Noeprene rubber was used for the simple composite model. Default neo-hookean data of rubber from ANSYS were used (Fig. 4.12). These materials were only used as conceptual possibilities, results

from OPENSEES modeling (Chapter 5) can determine desired hysteretic connection behavior characteristics which could then be approximated by composite connections of varying geometry and materials.

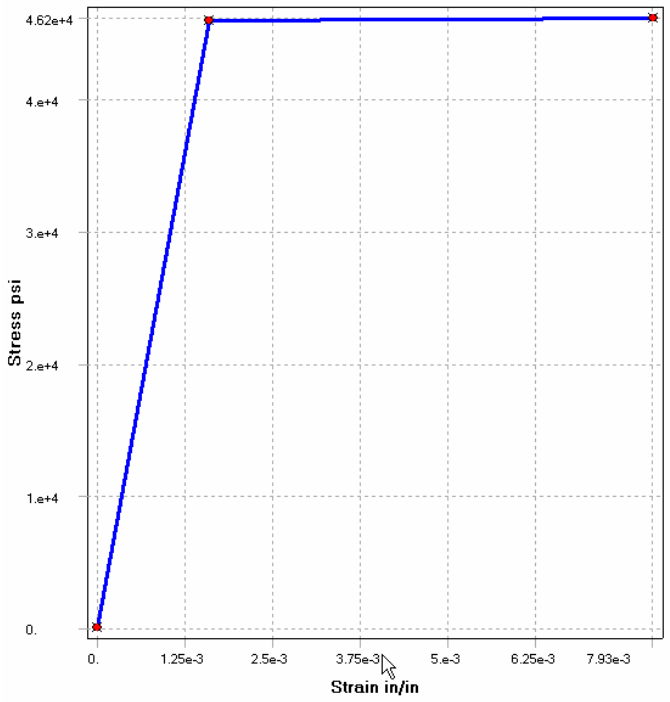

Figure 4.11 Bilinear kinematic hardening constitutive model for steel material.

For all three connections, boundary conditions assigned at the ends of connections were modified to determine their influence on behavior. The connection's surface attached to the frame was fully fixed. This was done by restraining all degrees-of-freedom of all nodes on the surface. The connection's surface attached to cladding panels was rotationally restrained or rotationally free (Fig. 4.13 - 4.15). Rotation was restrained by assigning zero out-of-plane displacements to the surface during the loading process. All three connections were subjected to quasi-static cycles of lateral displacements of different amplitudes (Fig. 4.16). To apply these cycles of displacements, the analysis

process was divided into 40 steps. Every 4 steps accommodated 1 cycle of displacement: zero to maximum, maximum to zero, zero to minimum and minimum to zero. Sub-steps for inelastic analysis were automatically defined by ANSYS with the maximum number of sub-steps set at 1000. Displacements were applied on the cladding surface of the connections. No vertical gravity load was included. Ultimate applied displacement was 1 inch. Large deformation was considered in the analysis. During the analysis, reaction forces, stresses and deformations were recorded.

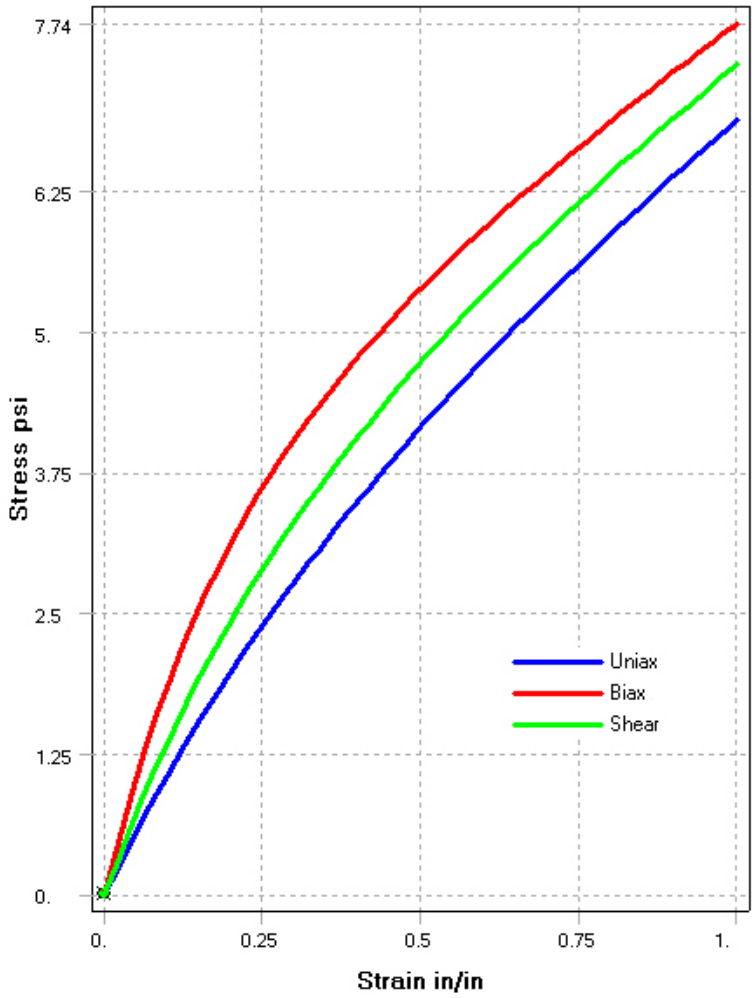

Figure 4.12 Neo-Hookean data of noeprene rubber used for composite connection

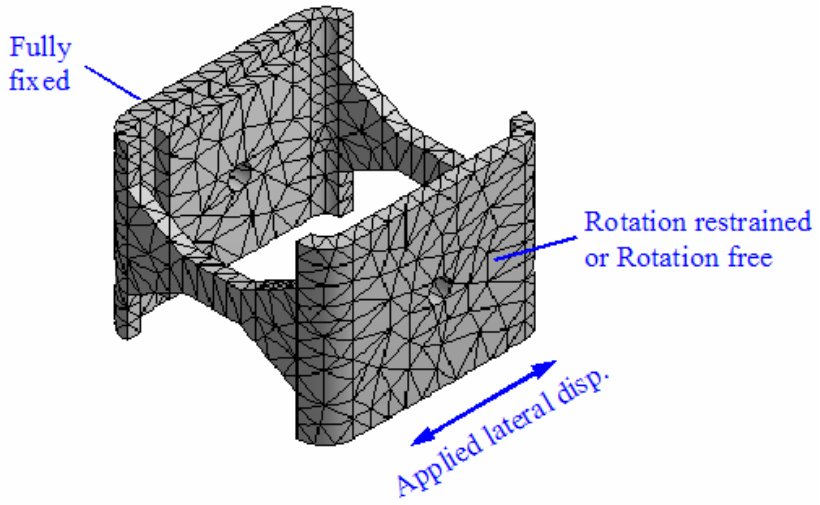

Figure 4.13 Boundary and loading condition for tapered tube connection

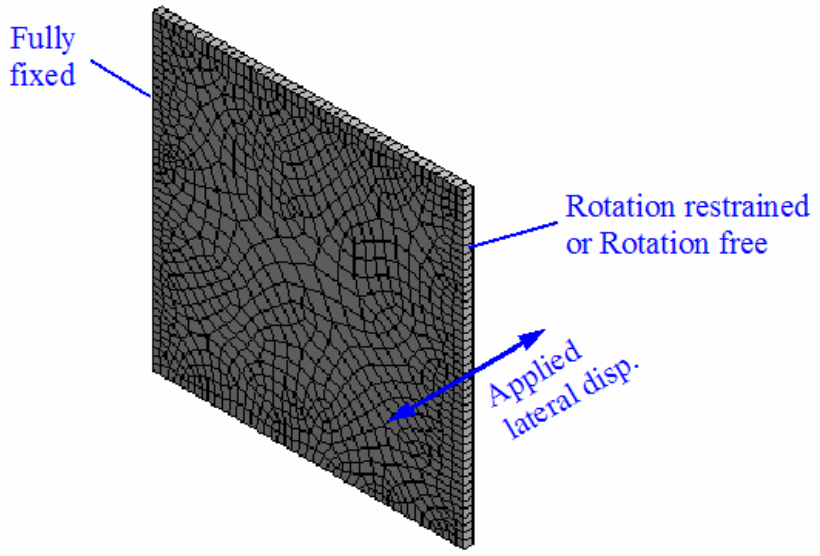

Figure 4.14 Boundary and loading condition for plate connection

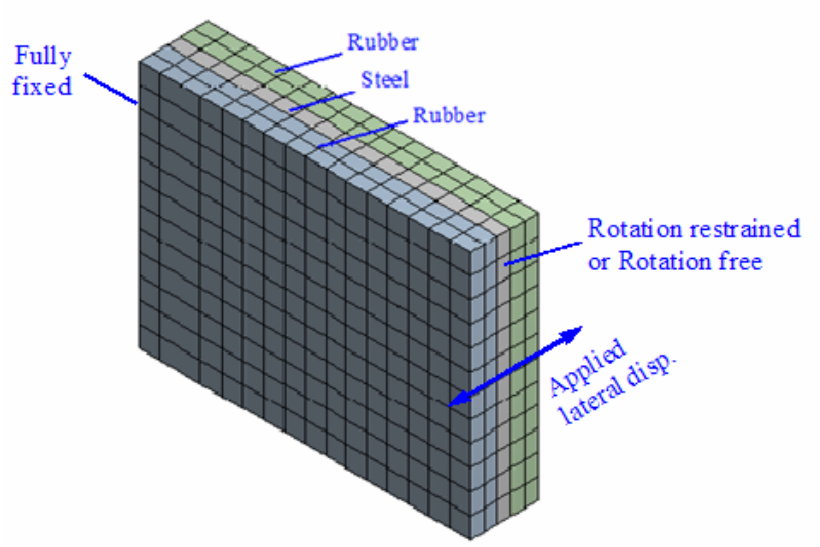

Figure 4.15 Boundary and loading condition for plate connection

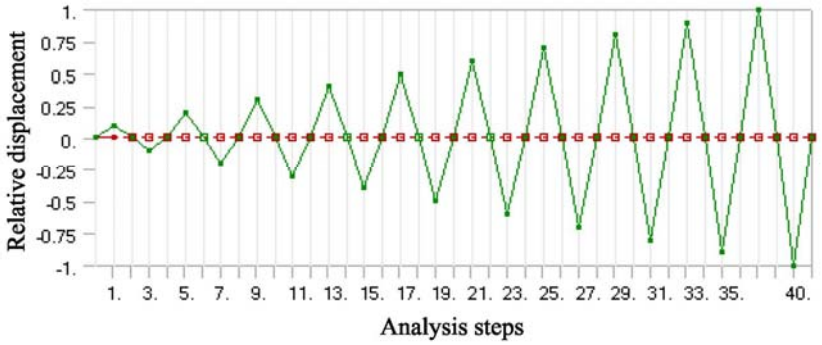

Figure 4.16 Input lateral displacement cycles.

4.3 Hysteretic responses of connections

Hysteretic responses of the tapered tube connection can be seen in Figure 4.16. Wide, stable loops were observed without stiffness degradation or strength deterioration. This confirmed the experimental results obtained by Pinelli et al. (1995) (see Figure 2.2). It was found that hysteretic behavior of connections depended on the rotational boundary condition at the cladding (comparing Figure 4.16a and b). In the case that rotation at the

cladding side of connection was restrained, shear reaction of the connection at displacement of 1 in (0.025 m) was 8.38 kips (37.3 kN). In the case that such rotation was free, the shear reaction of the connection at a displacement of 1 in was 3.77 kips (16.8 kN). Pinelli et al. (1995) reported experimental values of 4.2 kips (18.7 kN). At displacements of 0.4 in (0.01 m), all results (2 models and previous experimental work) indicate a shear of approximately 4 kips (17.8 kN). Hardening of the hysteretic response was significantly higher in the analytical model when rotation at cladding side of connection was restrained. Laboratory tests by Pinelli et al. (1995) resulted in a slight hardening effect up to a displacement of 1 in (0.025 m) between these two conditions, representing the difficulty of obtaining a truly fixed condition in an actual test setup. However, it is unclear what degree of fixity would be available in a full cladding system, so experimental testing of such components would be worthwhile. Further modeling could then include spring restraints rather than fully restrained boundary conditions to match the condition observed in testing. It is noted that the experimental results showed significant hardening when testing continued to 2.5 in (0.063 m).

Hysteretic responses of the plate connection can be seen in Figure 4.17. Note the different scales of the two graphs in Figure 4.17a and 4.17b. Much higher hardening effect than the case of tapered tube connection was observed when rotation at the cladding side of connection was restrained. The additional hardening was due to stress stiffening of the model. This effect normally occurs in thin structures with bending stiffness very small compared to axial stiffness and couples the in-plane and transverse displacements (ANSYS 11.0 help documentation). The effect was present only when large deformation effects were considered in the analysis. When large deformation effects

were considered, ANSYS accounted for the stress stiffening effect by adding an additional stiffness matrix to the regular non-linear stiffness matrix in order to give the total stiffness (ANSYS help 11.0 documentation).

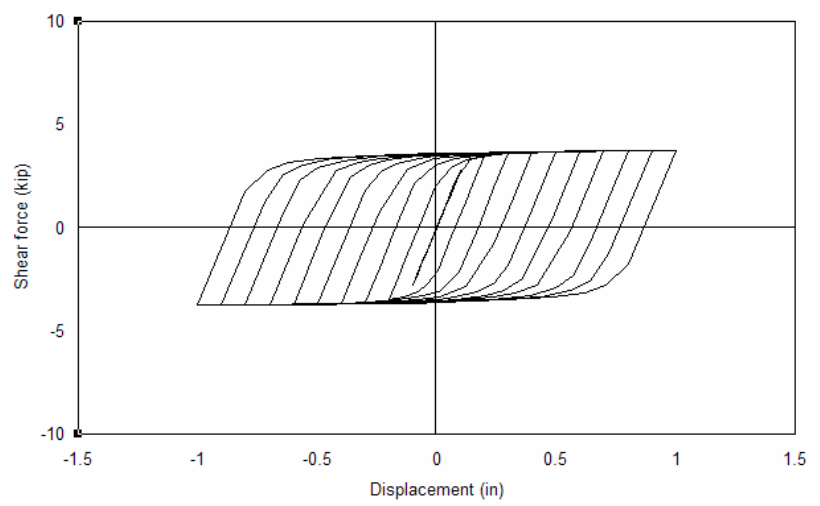

(a) Rotation free

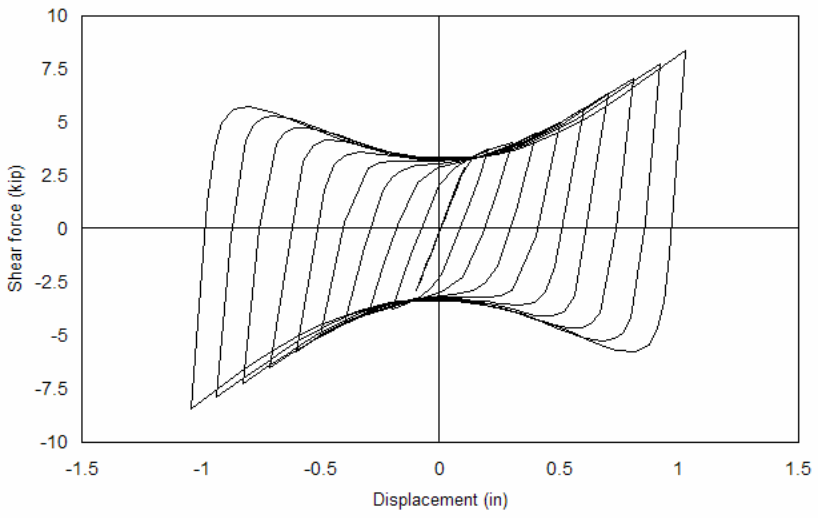

(b) Rotation restrained

Figure 4.17 Hysteretic behavior of tapered tube connection from ANSYS.

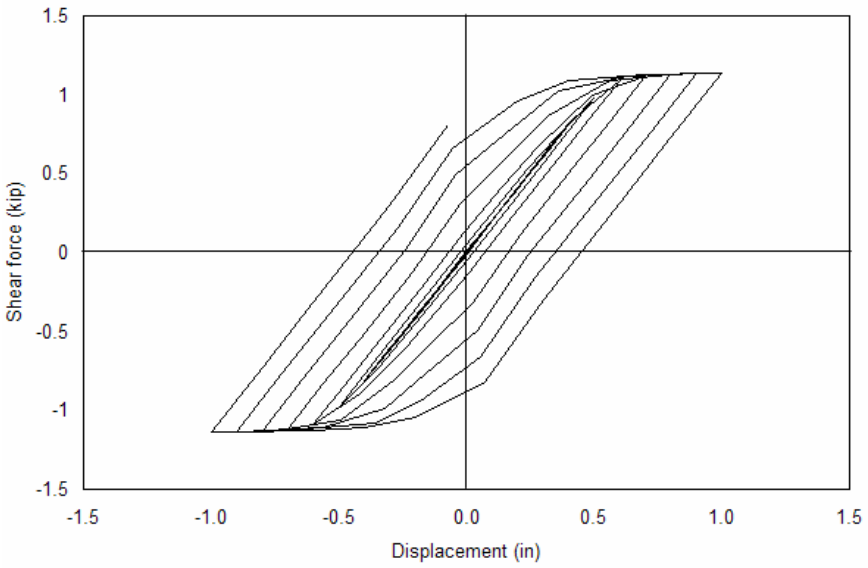

(a) Rotation free

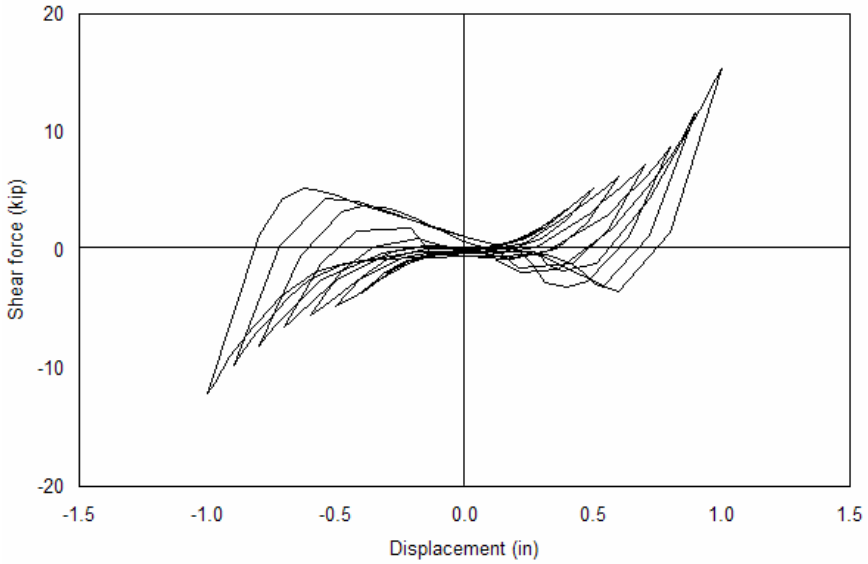

(b) Rotation restrained

Figure 4.18 Hysteretic behavior of plate connection from ANSYS.

Hysteretic responses of the simple composite connection can be seen in Figure 4.18. The composite connection provided wider loop with more hardening effect than the plate connection when they were both rotationally free. The hardening effect in the

simple composite connection was also significantly higher when rotation at cladding side of the connection was restrained.

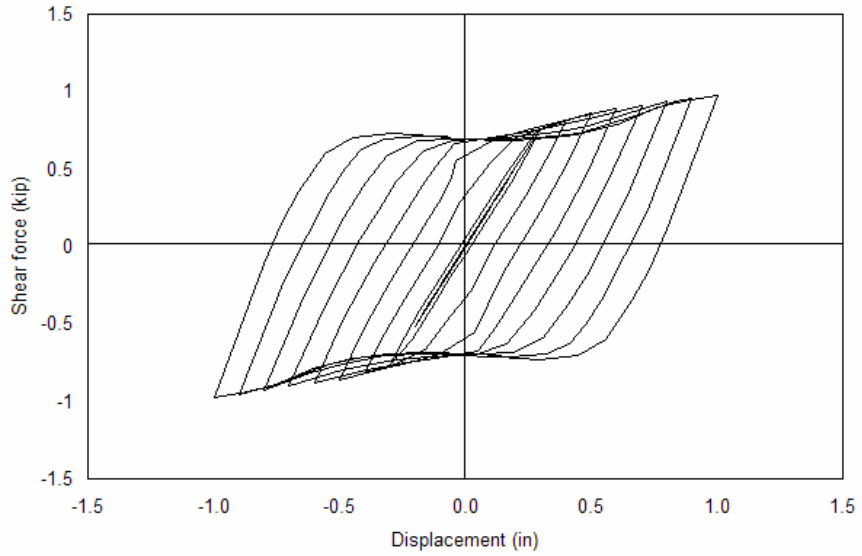

(a) Rotation free

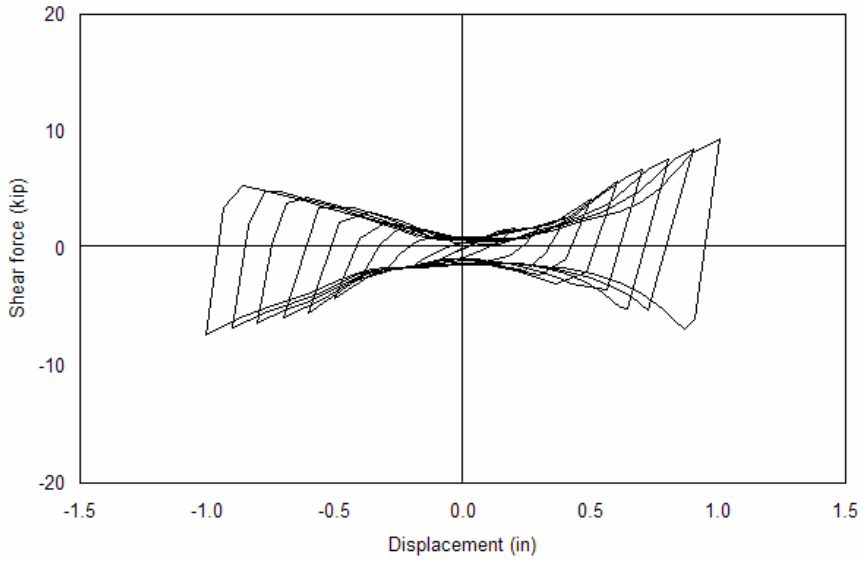

(b) Rotation restrained

Figure 4.19 Hysteretic behavior of simple composite connection from ANSYS.

Von-Misses stresses at connection deflections of 0.3 in (7.62 mm), 0.5 in (12.7 mm), 0.7 in (17.78 mm) and 1 in (25.4 mm) were shown in Figure 4.20 - 4.35. For the tapered tube connection, when rotation at the cladding side of connection was not restrained (Fig. 4.20 - 4.23), at the connection deflection of 0.3 in, yielding stresses (46 ksi) (317.2 Mpa) were not observed at most locations (Fig. 4.20). High stresses were observed near the tapered locations of the beams. When the deflection of connection increased, stresses increased and yielding stresses started to appear near the tapered locations of the beams. At the connection deflection of 1 in (25.4 mm), after yielding occurred near the tapered locations of the beams, yielding stresses also appeared near the ends of the beams (Fig. 4.23).

For the tapered tube connection, when rotation at the cladding side of connection was restrained (Fig. 24 - 4.27), locations of yielding stresses were different with the case that such rotation was not restrained. Yielding stresses appeared earlier. At the connection deflection of 0.3 in (7.62 mm), yielding stresses (46 ksi) (317.2 Mpa) started to appear near the ends of the beams (Fig. 4.24). At the deflection of 0.5 in (12.7 mm), yielding stresses were observed at most areas near the ends of the beams. After yielding occurred at the end of the beam, it developed to the middle of the beam (Fig 4.27).

For the plate connection, when rotation at the cladding side of connection was not restrained (Fig. 4.28 - 4.31), at the deflection of 0.3 in (7.62 mm), high stress areas were near the fixed end of the plate. Stresses did not reach yielding point yet. When deflection was 0.5 in (12.7 mm), yielding stresses appeared in similar areas. When deflection continued to increase to 1 in (25.4 mm), stresses increased and areas of highest stresses were still located near the fixed end of the plate.

For the plate connection, when rotation at the cladding side of connection was restrained (Fig. 4.32 - 4.35), at the deflection of 0.3 in (7.62 mm), high stress areas were observed at both ends of the connection. Stresses reduced uniformly from 2 ends to the middle of the plate. At the deflection of 0.5 in (12.7 mm), yielding occurred. Yielding stresses were located near the fixed end of the connection. At the deflection of 0.7 in (17.78 mm), yielding stresses were still observed near the fixed end of the connection. There was a slight reduction in maximum stress from 54.2 ksi (373.7 Mpa) to 53.6 ksi (369.6 Mpa). At the deflection of 1 in (25.4 mm), yielding stresses developed from the fixed end of the connection to more than two-third of the total length of the connection. Maximum stress was reduced from 53.6 ksi (369.6 Mpa) at the deflection of 0.7 in (17.78 mm) to 46.9 ksi (323.4 Mpa) at the deflection of 1 in (25.4 mm).

4.4 Conclusion

A method to obtain hysteretic behavior of different types of connections using 3-dimensional FEM models in ANSYS was presented. Analytical results indicated that response of connections is significantly dependent on rotational boundary conditions at the ends of connections. Further investigations on the actual rotational conditions of connections in a full system by testing and using spring restraints in analytical models rather than fully restrained boundary conditions would be worthwhile. Obtained hysteretic responses were then input into structural models in OPENSEES of the reference structure to examine the effectiveness of hysteretic energy dissipating connections.

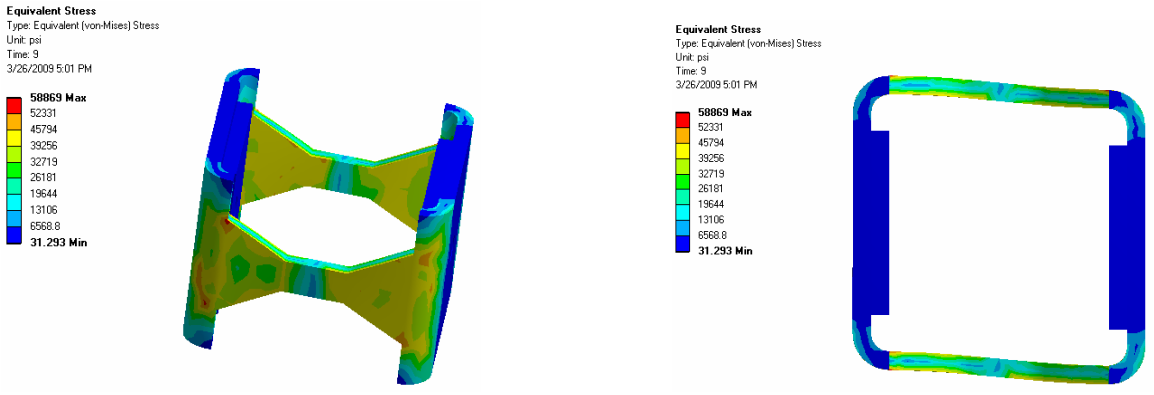

Figure 4.20 Von-Misses stresses of tapered tube connection at cladding deflection of 0.3 in, rotation free.

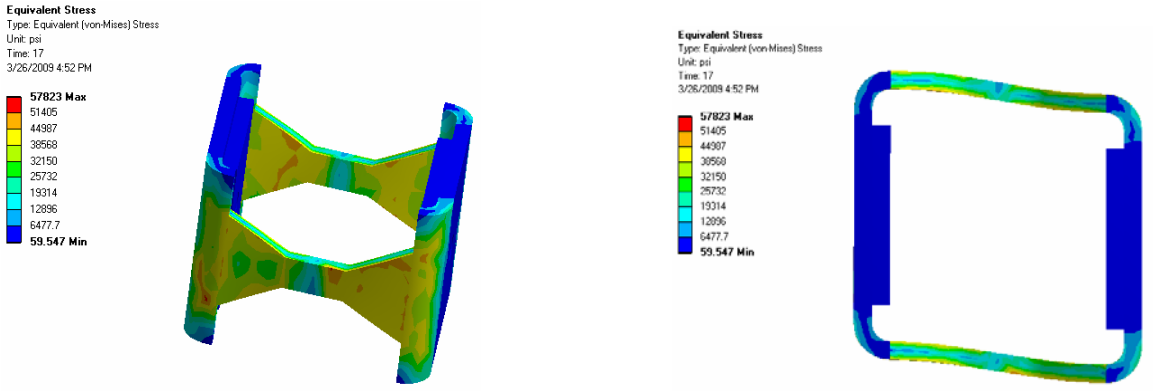

Figure 4.21 Von-Misses stresses of tapered tube connection at cladding deflection of 0.5 in, rotation free.

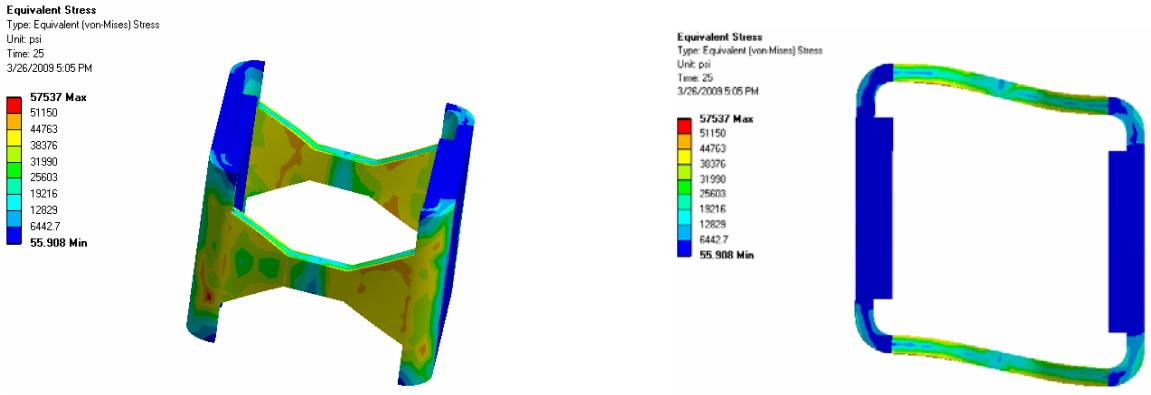

Figure 4.22 Von-Misses stresses of tapered tube connection at cladding deflection of 0.7 in, rotation free.

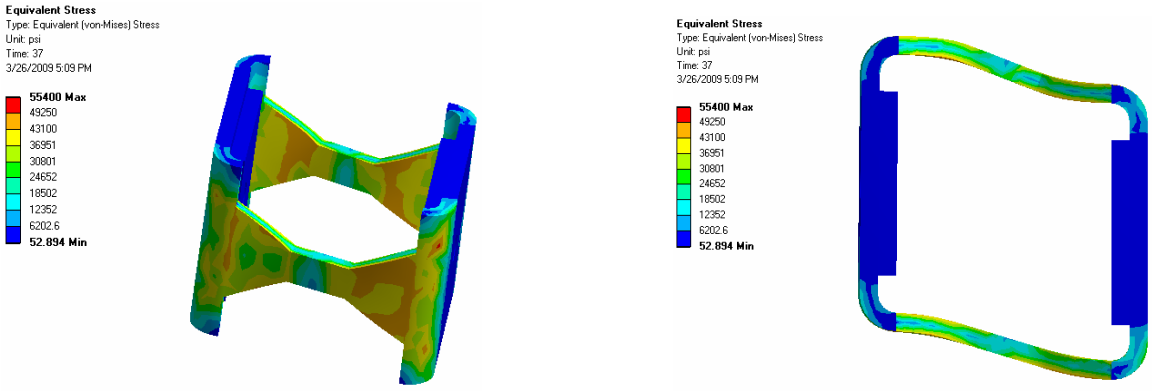

Figure 4.23 Von-Misses stresses of tapered tube connection at cladding deflection of 1 in, rotation free.

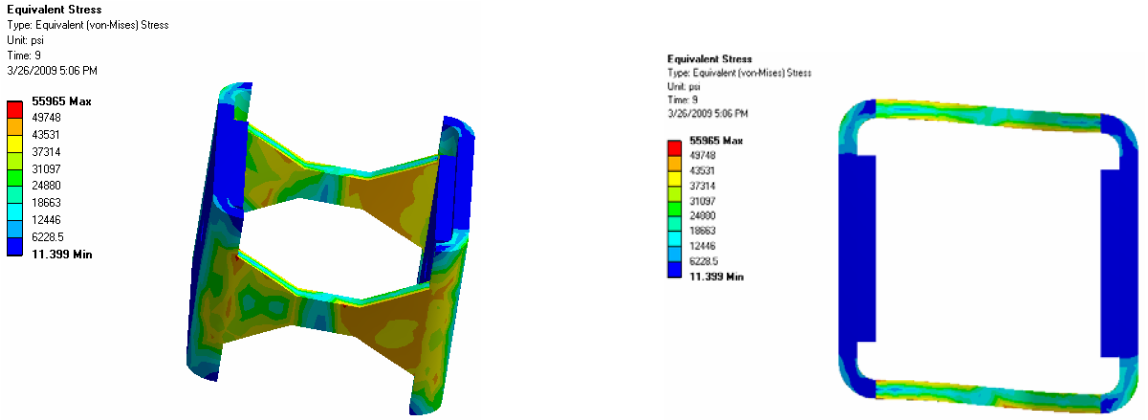

Figure 4.24 Von-Misses stresses of tapered tube connection at cladding deflection of 0.3 in, rotation restrained.

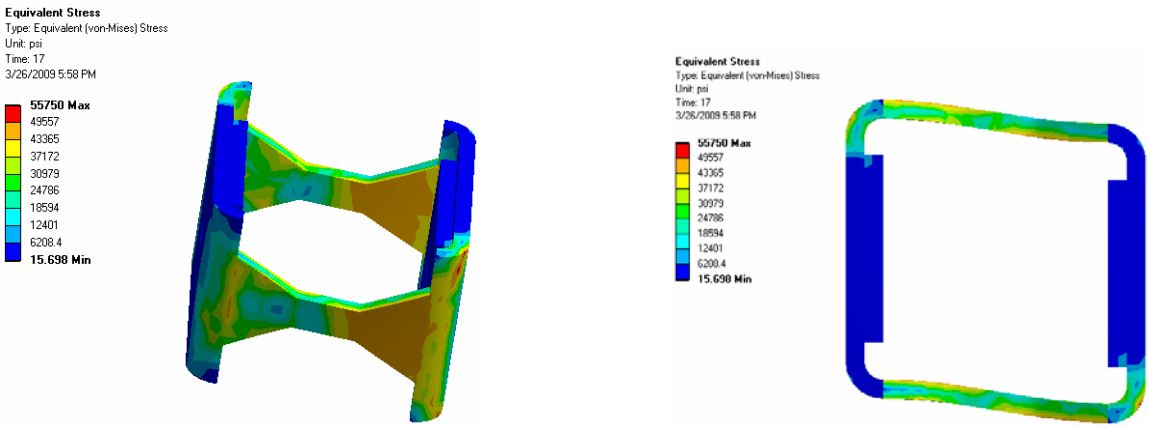

Figure 4.25 Von-Misses stresses of tapered tube connection at cladding deflection of 0.5 in, rotation restrained.

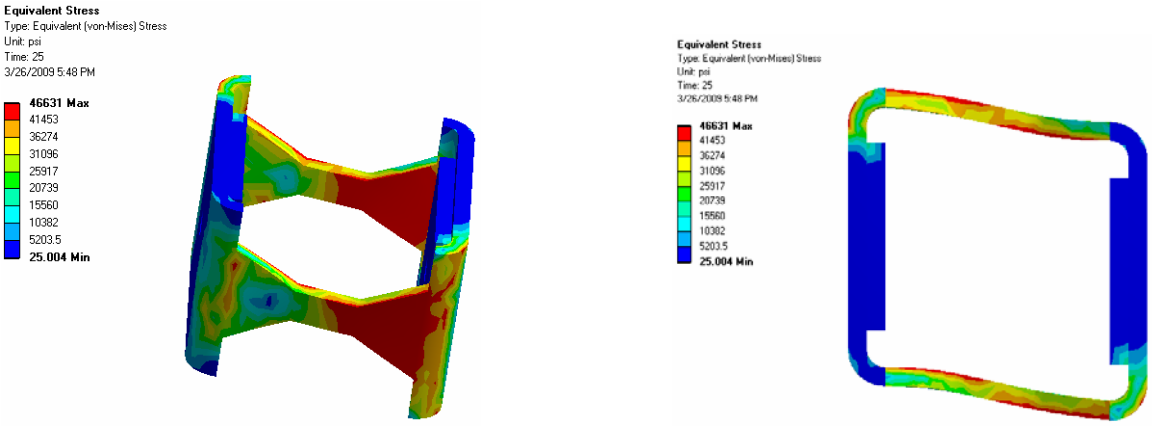

Figure 4.26 Von-Misses stresses of tapered tube connection at cladding deflection of 0.7 in, rotation restrained.

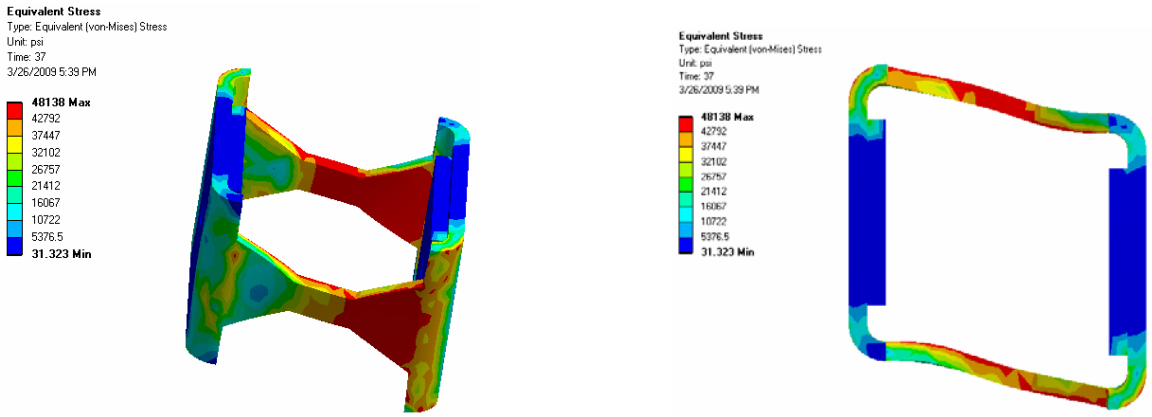

Figure 4.27 Von-Misses stresses of tapered tube connection at cladding deflection of 1 in, rotation restrained.

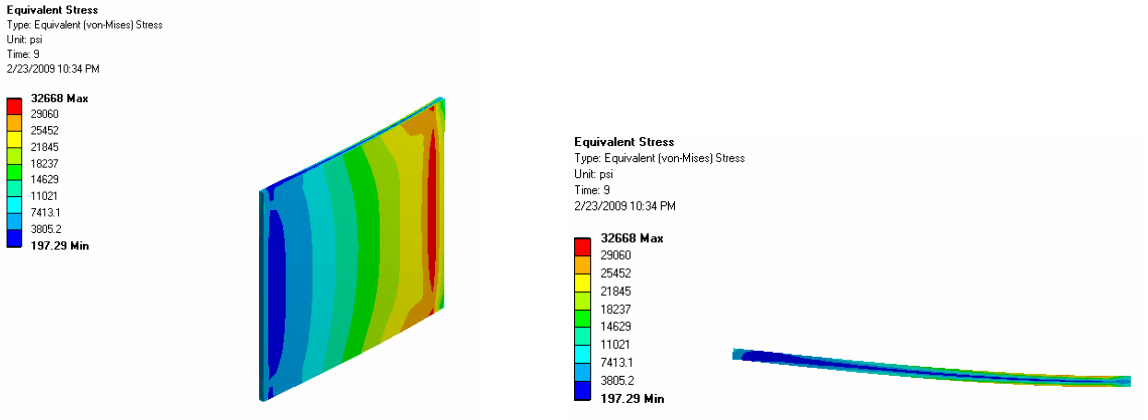

Figure 4.28 Von-Misses stresses of plate connection at cladding deflection of 0.3 in, rotation free.

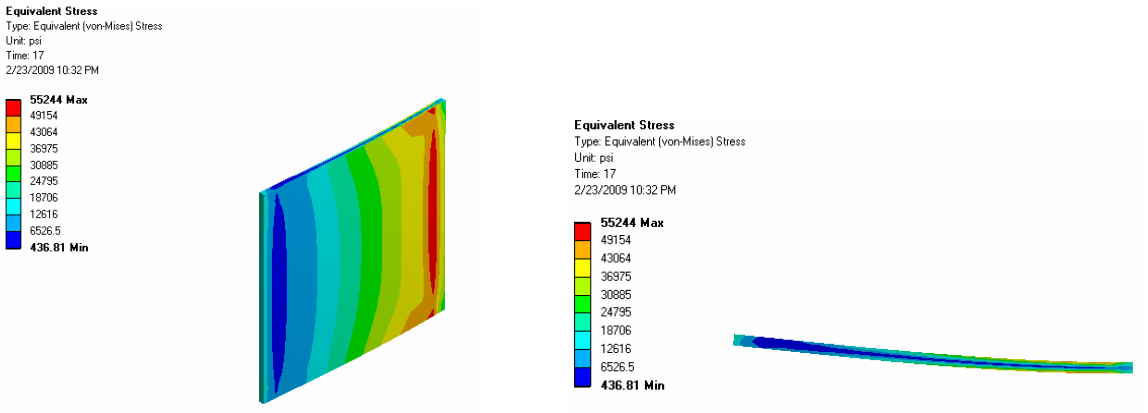

Figure 4.29 Von-Misses stresses of plate connection at cladding deflection of 0.5 in, rotation free.

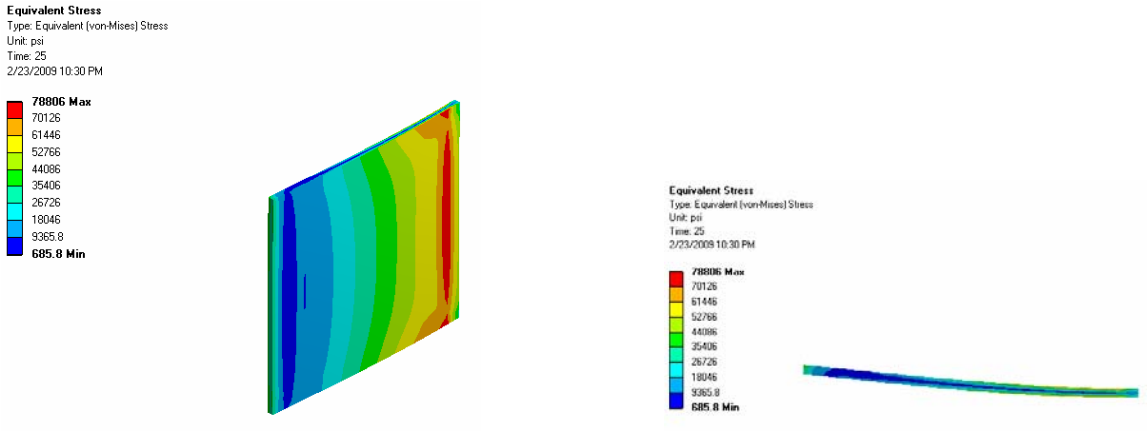

Figure 4.30 Von-Misses stresses of plate connection at cladding deflection of 0.7 in, rotation free.

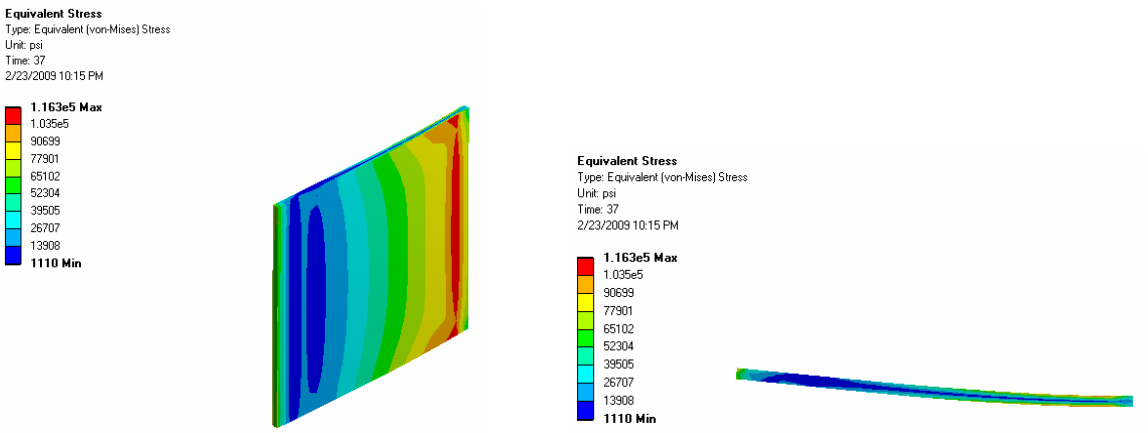

Figure 4.31 Von-Misses stresses of plate connection at cladding deflection of 1 in, rotation free.

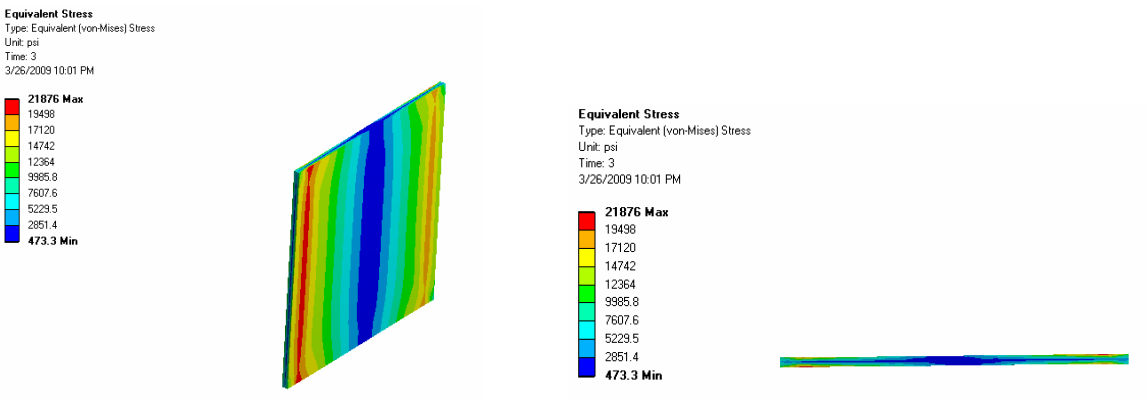

Figure 4.32 Von-Misses stresses of plate connection at cladding deflection of 0.3 in, rotation restrained.

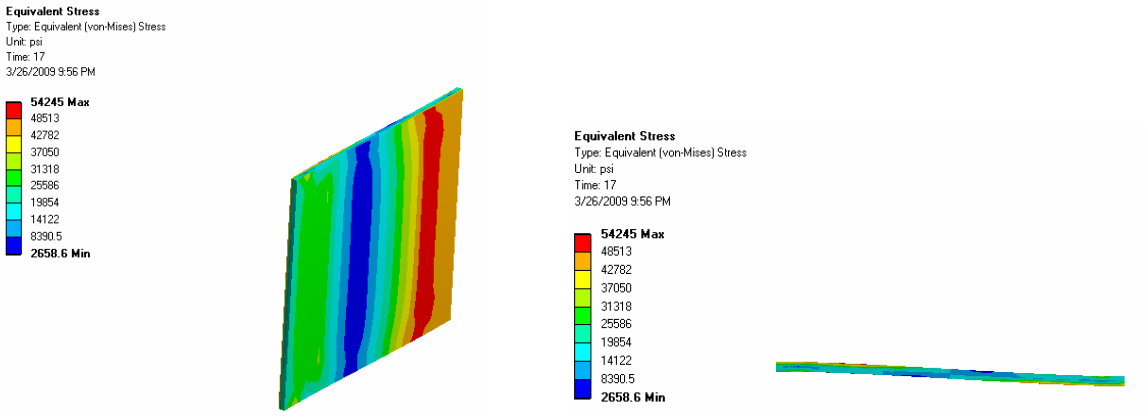

Figure 4.33 Von-Misses stresses of plate connection at cladding deflection of 0.5 in, rotation restrained.

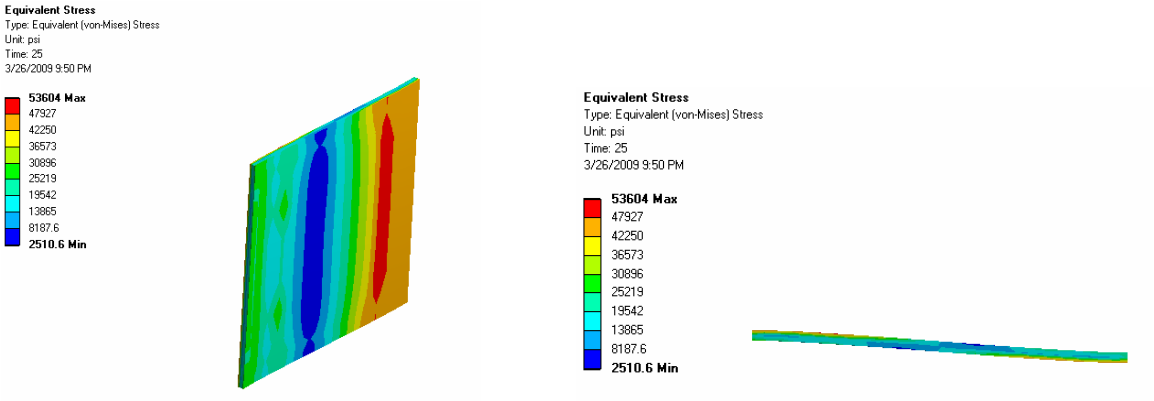

Figure 4.34 Von-Misses stresses of plate connection at cladding deflection of 0.7 in, rotation restrained.

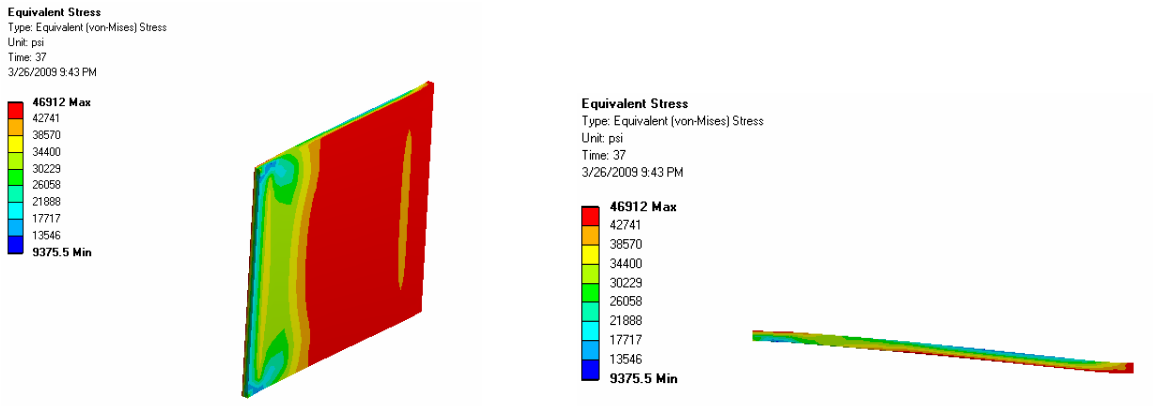

Figure 4.35 Von-Misses stresses of plate connection at cladding deflection of 1 in, rotation restrained.

CHAPTER 5

EFFECTS OF HYSTERETIC ENERGY DISSIPATION CONNECTIONS ON THE SAC 3-STORY BUILDING

5.1 Introduction

This chapter presents a non-linear analysis of the reference frame including hysteretic behavior of cladding-to-frame connections to investigate the effectiveness of total energy dissipation in connections under earthquake loading. Hysteretic behavior of connections obtained from ANSYS analysis (Chapter 4) was input into a non-linear SAC 3-story frame model developed in OPENSEES. Both geometric and material non-linearity of the frame were considered. Results from non-linear time history analysis of the frame without cladding-to-frame connections were calibrated to Ohtori et al. (2004) to assure the validity of the analysis model. Connections were included in the model as non-linear springs connecting coincident frame and cladding mass joints which were defined as having equivalent hysteretic behavior to that obtained from the FEM analysis. A series of hypothetical connection response (defined through hysteretic behavior characteristics) were also examined for their effects on seismic responses of the structure. Analysis results have demonstrated the potential to utilize hysteretic energy dissipation connections to reduce the response of structures subjected to earthquakes.

5.2 Non-linear model of the SAC 3-Story building

Non-linear analysis of structures subjected to earthquakes is necessary because of the fact that large deformations and inelastic material behaviors are expected to occur in the structures during earthquakes. A non-linear model of the SAC 3-story building was developed in OPENSEES - an advanced computer program for earthquake simulation.

The model was able to take into account both geometric and material non-linearity and is extremely flexible in allowing true hysteretic behavior of elements.

Details of the SAC 3-story building were described in Chapter 3. Frame members were modeled by non-linear frame elements with 5 integration points along each element to account for geometric non-linearity. This frame element is flexibility-based using force interpolation functions instead of displacement interpolation functions as commonly used in a stiffness-based frame element. This element has several advantages over the stiffness-based element including less discretization errors and exactly satisfied governing equations. Background and formulation of this element can be found in Neuenhofer and Filippou (1997). The command to define this element is as follows (after OPENSEES Command Language Manual):

"element nonlinearBeamColumn $eleTag $iNode $jNode $numIntgrPts $secTag $transfTag <-mass $massDens> <-iter $maxIters $tol>"

In which:

- $eleTag: unique element object tag
- $iNode $jNode: end nodes
- $numIntgrPts: number of integration points along the element.
- $secTag: identifier for previously-defined section object
- $transfTag: identifier for previously-defined coordinate-transformation object
- $massDens: element mass density (per unit length), from which a lumped-mass matrix is formed (optional, default=0.0)

- $maxIters maximum number of iterations to undertake to satisfy element compatibility (optional, default=1)
- $tol tolerance for satisfaction of element compatibility (optional, default=10^{-16})

To model material non-linear behavior, cross sections of frame members were broken down into quadrilateral patches. There were 64 patches for each flange and 32 patches for the web. Patches were then assigned uni-axial bilinear kinematic hardening material behavior with parameters commonly used for structural steel. This was one of the "fiber" methods to model cross sections in OPENSEES. Elastic modulus of steel was 29,000 ksi (199,947 Mpa). Tangent modulus was 29 ksi (199.95 Mpa). Yield stress was 50 ksi (344.7 Mpa). Poisson's ratio was 0.3.

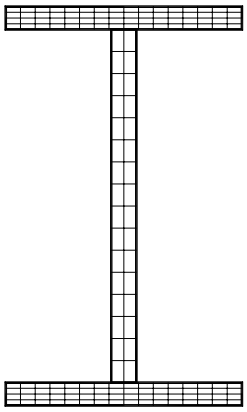

Figure 5.1 Quadrilateral patches of frame member cross section.

To ensure the validity of the modeling of the structure, the non-linear frame was analyzed with El Centro earthquake ground motion previously described in Chapter 3. Results were compared with Ohtori's analysis (2004). It is seen that results from OPENSEES analysis and Ohtori's analysis are in good agreement (Table 5.1).

Table 5.1 Calibration of results for the OPENSEES non-linear frame.

Structural Responses	OPENSEES	Ohtori et. al (2004)
Peak story drift ratio	0.014	0.015
Peak level acceleration (in/s^2)	285.5	257.5
Peak base shear (Kip)	1116.5	1137.5

5.3 Non-linear springs representing hysteretic behavior of connections

To input into the frame model, hysteretic behavior of connections was represented by non-linear springs. Non-linear stiffness of a spring which is a function of displacement was defined so that when the spring was subjected to the same load as the connection in the FEM model (Chapter 4) an equivalent hysteretic response can be obtained.

To model the non-linear spring which provided the equivalent hysteretic response with the connection, OPENSEES truss element was used. The truss element only has axial degree-of-freedom. Behavior of a truss element is defined by its cross sectional area and assigned uni-axial material behavior. Two material constitutive laws were applied to obtain equivalent hysteretic responses. The first one was the OPENSEES "Steel 02" material model. This material model was employed to represent hysteretic behavior of the tapered tube connection without rotation restrained. Parameters of "Steel 02" material model are as follows (after OPENSEES Command Language Manual (Fig. 5.2)):

- Fy: yield strength
- E: initial elastic tangent
- b: strain-hardening ratio
- R0, cR1, cR2: parameter to control the transition from elastic to plastic branches.

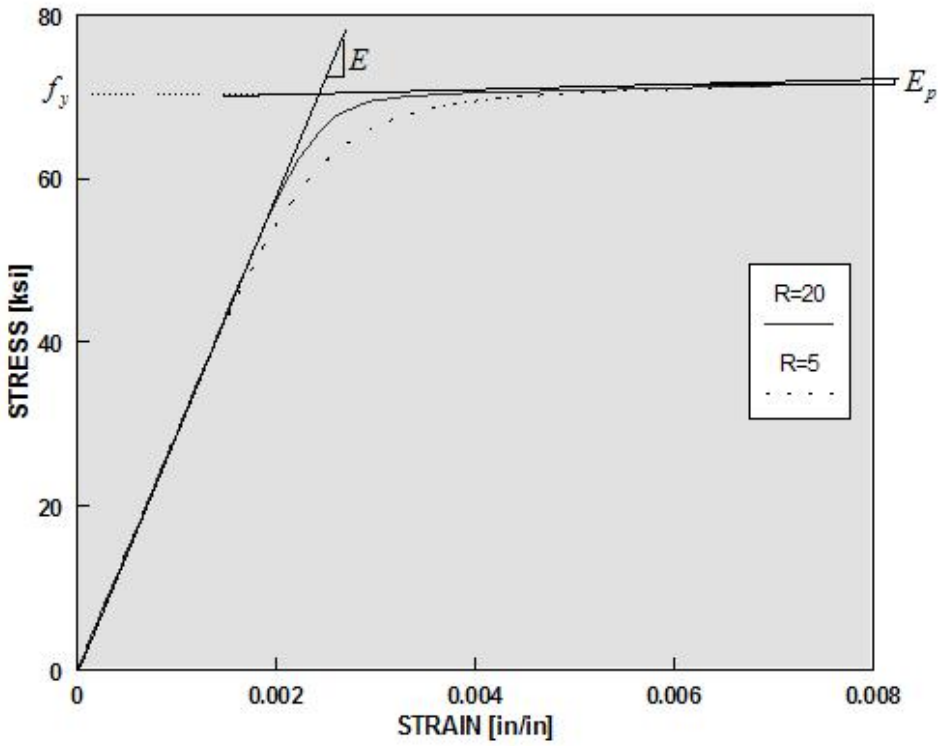

Figure 5.2 "Steel 02" material model (from OPENSEES).

Parameters of the "Steel 02" material model were varied to match hysteretic response from the non-linear spring with hysteretic response from FEM analysis for the tapered tube connection with free rotations at cladding side. Responses of the non-linear spring with different "Steel 02" material parameter sets shown in Table 5.2 can be seen from Figure 5.3 to Figure 5.7.

Table 5.2 "Steel 02" parameter sets.

Parameter set	Steel02_01	Steel02_02	Steel02_03	Steel02_04	Steel02_05
Fy (ksi)	46	46	46	46	46
E (ksi)	5000	4200	4200	4200	4000
b	0.01	0.01	0.01	0.01	0.006
R0	20	25	30	35	35
cR1	0.925	0.925	0.925	0.925	0.925
cR2	0.15	0.15	0.15	0.15	0.1
Cross-sectional area (in^2)	0.08	0.08	0.08	0.08	0.08

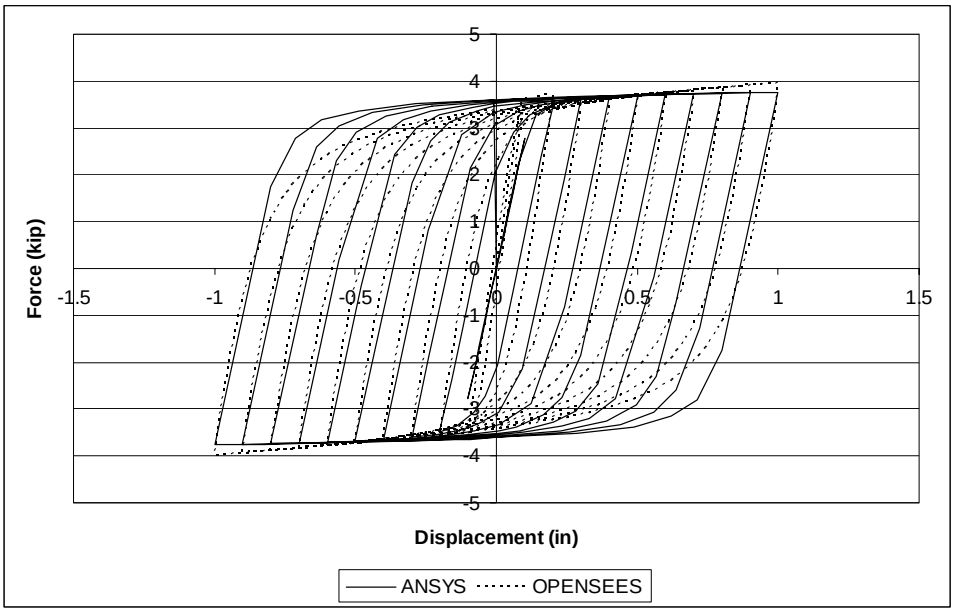

Figure 5.3 Response of non-linear spring with parameter set Steel02_01.

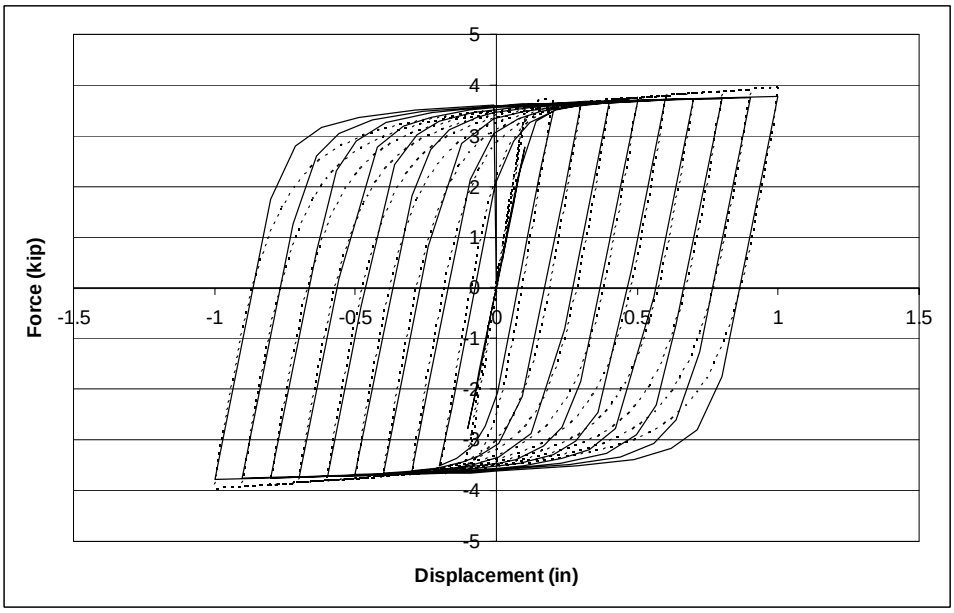

Figure 5.4 Response of non-linear spring with parameter set Steel02_02.

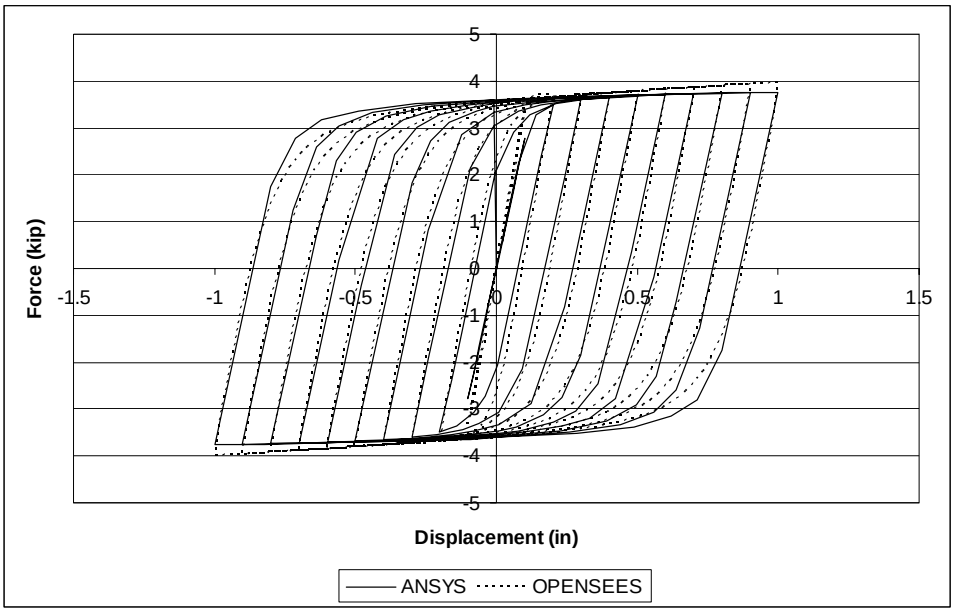

Figure 5.5 Response of non-linear spring with parameter set Steel02_03.

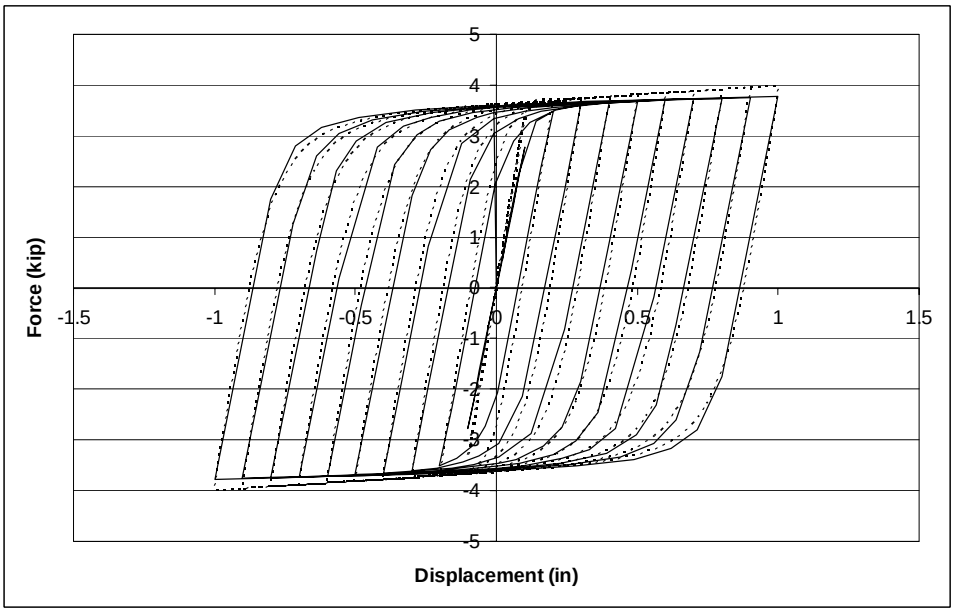

Figure 5.6 Response of non-linear spring with parameter set Steel02_04.

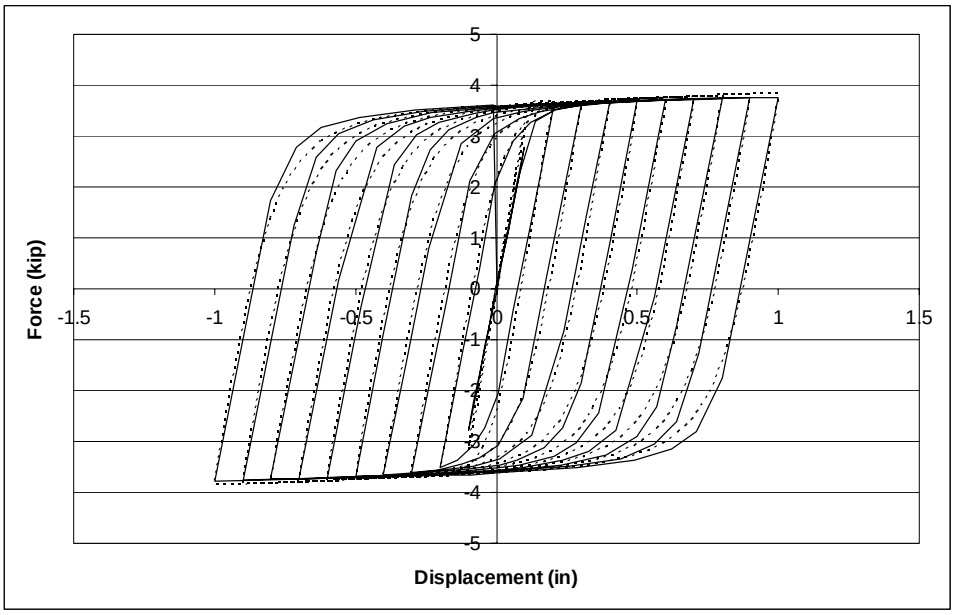

Figure 5.7 Response of non-linear spring with parameter set Steel02_05.

The second constitutive law was the OPENSEES "hysteretic material" model. Parameters of this material model are as follows (after OPENSEES Command Language Manual (Fig. 5.8)):

- s1p,e1p: stress and strain (or force & deformation) at first point of the envelope in the positive direction
- s2p, e2p: stress and strain (or force & deformation) at second point of the envelope in the positive direction
- s3p, e3p: stress and strain (or force & deformation) at third point of the envelope in the positive direction (optional)
- s1n, e1n: stress and strain (or force & deformation) at first point of the envelope in the negative direction

- s2n, e2n: stress and strain (or force & deformation) at second point of the envelope in the negative direction
- s3n, e3n: stress and strain (or force & deformation) at third point of the envelope in the negative direction (optional)
- pinchX: pinching factor for strain (or deformation) during reloading
- pinchY: pinching factor for stress (or force) during reloading

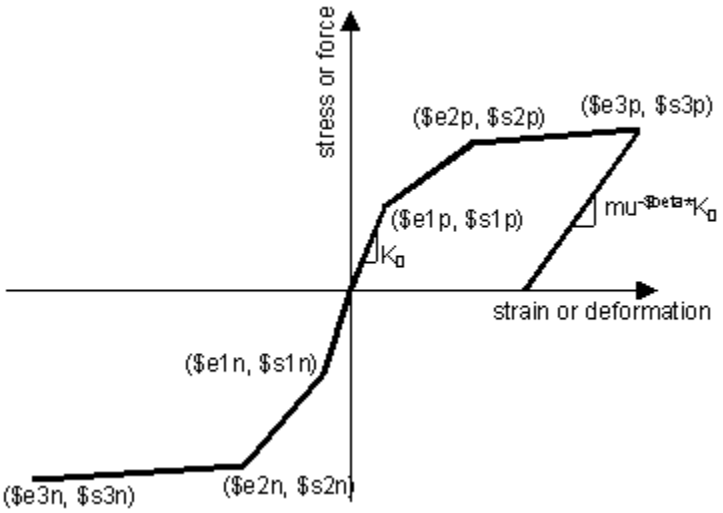

Figure 5.8 "Hysteretic material" model (from OPENSEES)

Parameters of the "hysteretic material" model were varied to match hysteretic response from the non-linear spring with hysteretic response from FEM analysis of the tapered tube connection with rotations at cladding side restrained. Responses of the non-linear spring with different "hysteretic material" parameter sets shown in Table 5.3 can be seen from Figure 5.9 to Figure 5.13.

Table 5.3 "Hysteretic material" parameter sets.

Parameter set	Hys01	Hys02	Hys03	Hys04	Hys05
s1p (kip)	2.8849	2.8849	2.8849	2.8849	2884.9
e1p (in)	0.1	0.1	0.1	0.1	0.1
s2p (kip)	3.3718	3.3718	3.3551	3.3551	3355.1
e2p (in)	0.126	0.126	0.145	0.145	0.145
s3p (kip)	3.4193	3.4193	8.3821	8.3821	8382.1
e3p (in)	0.195	0.195	1.03	1.03	1.03
s1n (kip)	-2.8849	-2.8849	-2.8849	-2.8849	-2884.9
e1n (in)	-0.1	-0.1	-0.1	-0.1	-0.1
s2n (kip	-3.3718	-3.3718	-3.3551	-3.3551	-3355.1
e2n (in)	-0.126	-0.126	-0.145	-0.145	-0.145
s3n (kip)	-3.4193	-3.4193	-8.3821	-8.3821	-8382.1
e3n (in)	-0.195	-0.195	-1.03	-1.03	-1.03
pinchX	1	0.2	0.2	0.1	0.1
pinchY	1	0.8	0.8	0.8	0.6
Cross-sectional area (in^2)	1	1	1	1	1

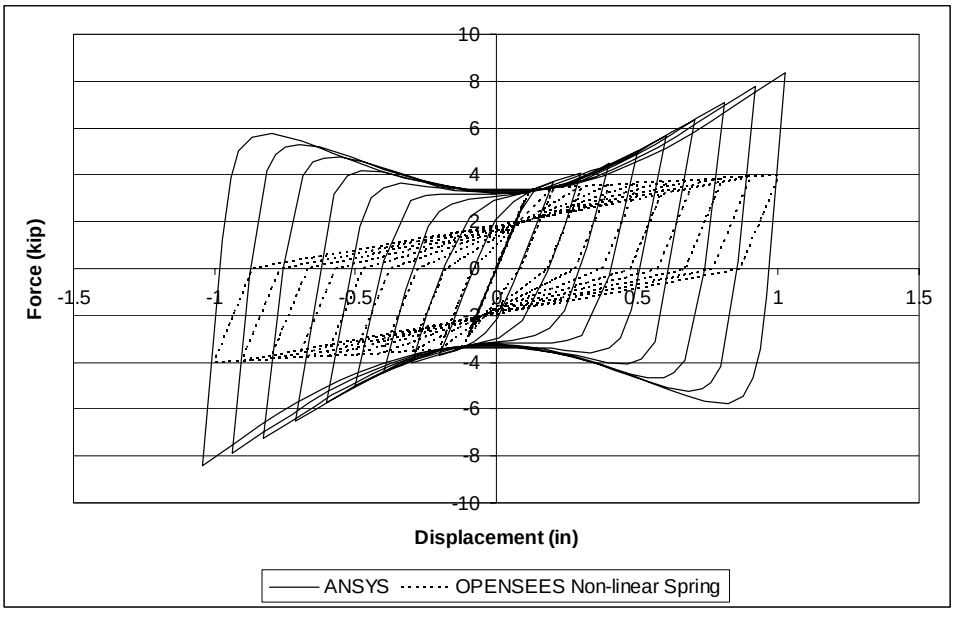

Figure 5.9 Response of non-linear spring with parameter set Hys01.

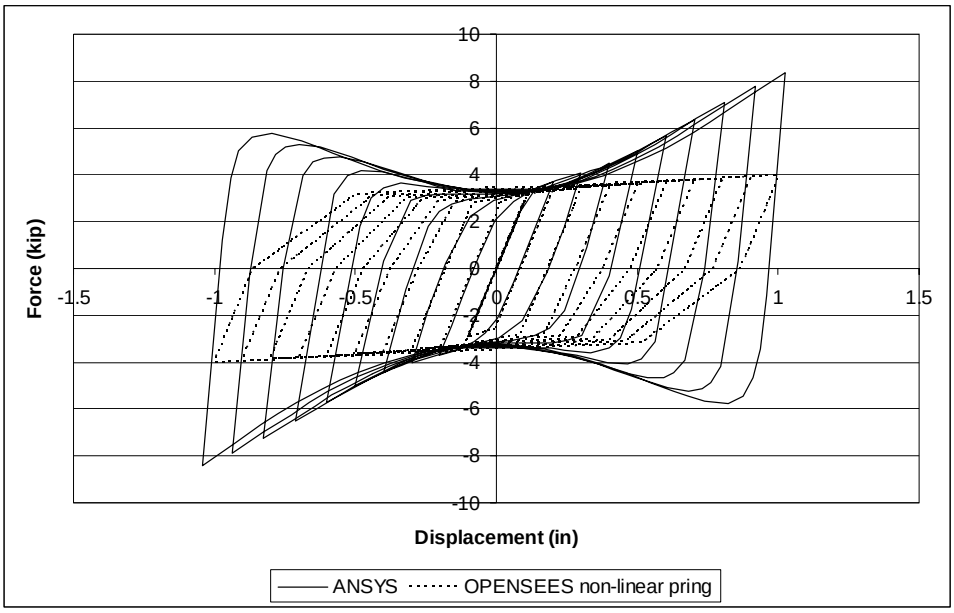

Figure 5.10 Response of non-linear spring with parameter set Hys02.

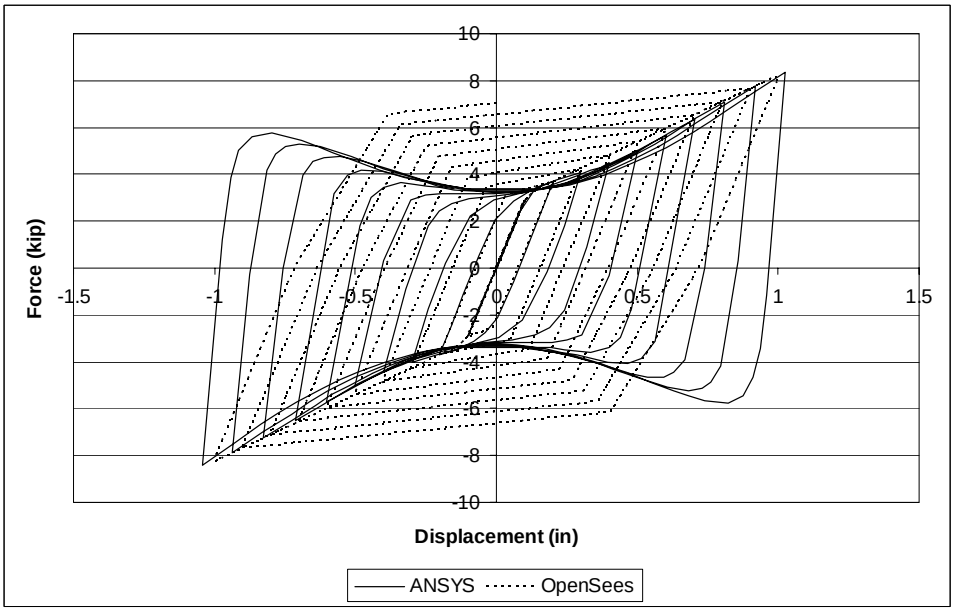

Figure 5.11 Response of non-linear spring with parameter set Hys03.

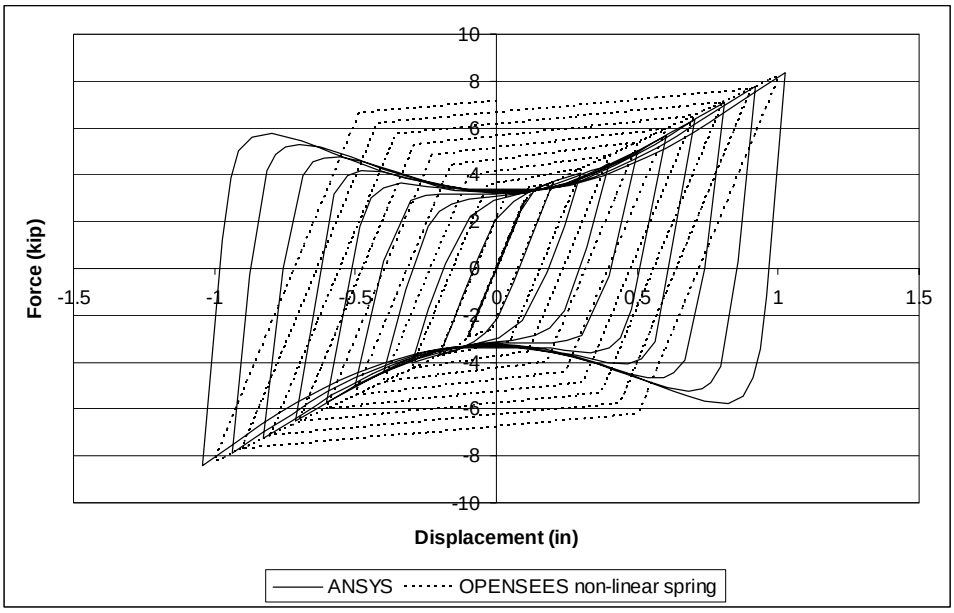

Figure 5.12 Response of non-linear spring with parameter set Hys04.

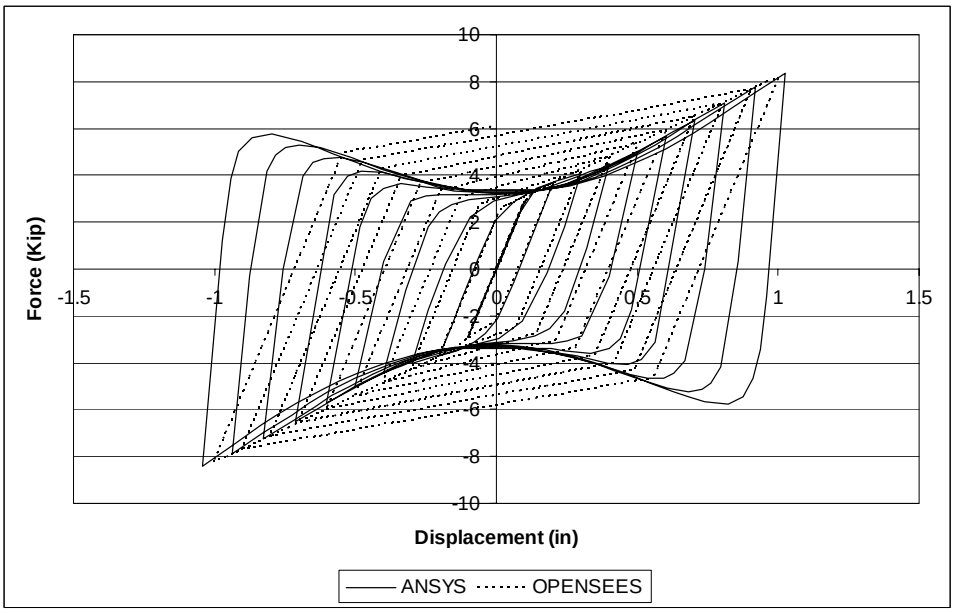

Figure 5.13 Response of non-linear spring with parameter set Hys05.

There were limitations in this material model to represent non-linear effects of this particular hysteretic response. Due to short of time of this research, behavior of the rotation restrained connection with higher hardening and pinching effects than the rotation free connection was not included in further analysis.

Response from the non-linear spring with parameter set Steel02_05 was closest to the hysteretic behavior of tapered tube connection from ANSYS analysis. This parameter set was used to define the non-linear spring representing the tapered tube connection in the reported OPENSEES models.

5.4 Non-linear analysis of the SAC 3-story building including hysteretic behavior of cladding-to-frame connections

To investigate the effectiveness of hysteretic energy dissipation connections on seismic structural responses, non-linear springs with behavior as in Figure 5.7, representing tapered tube connections with a free condition at the cladding, were incorporated into the OPENSEES non-linear frame model. The number of truss elements representing non-linear springs at each joint was equal to number of connections at each joint (Fig. 5.14). A single connection was assumed for each piece of cladding being attached at that joint. Cladding masses were assigned at the free ends of the truss elements. At joints having more than 1 truss element, different truss elements connected the same two nodes - the frame joint and the cladding joint.

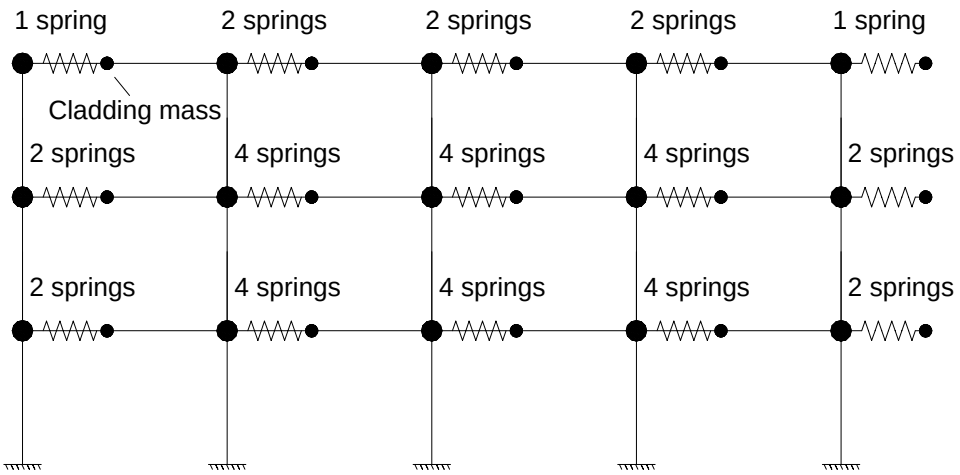

Figure 5.14 Input non-linear springs into the frame model.

There were totally 27 frame elements for beams and columns and 40 elements for non-linear springs. The frame was analyzed with El Centro earthquake ground motion previously described in Chapter 3. Newmark integration method was used with time step of 0.01s. Analysis results with rigid and tapered tube connections were compared in Table 5.4. Analysis results indicated that structural responses were not significantly reduced when tapered tube connections were included. This was because the connection stiffness was initially too high to be effective. Time history plots of absolute cladding displacements and absolute frame displacements at 3rd floor are shown in Figure 5.15. Cladding deflections (relative displacements between steel frame and cladding) at different floors were shown in Figure 5.16. The maximum cladding deflection was only 0.52 in (13.2 mm) resulting in moderate yielding in connections (see yielding in connection at 0.5 in (13.2 mm) deflection in Figure 4.21). This led to insignificant energy dissipation within the cladding as it was also too stiff to be effective as a MTMD (see Chapter 3). It is seen that this connection was not optimized for this structure.

Table 5.4 Analysis results with and without hysteretic connections

Structural Responses	Rigid connections	Tapered tube connections
Peak story drift ratio	0.014	0.014
Peak level acceleration (in/s^2)	285.5	283.2
Peak base shear (Kip)	1116.5	1108.1

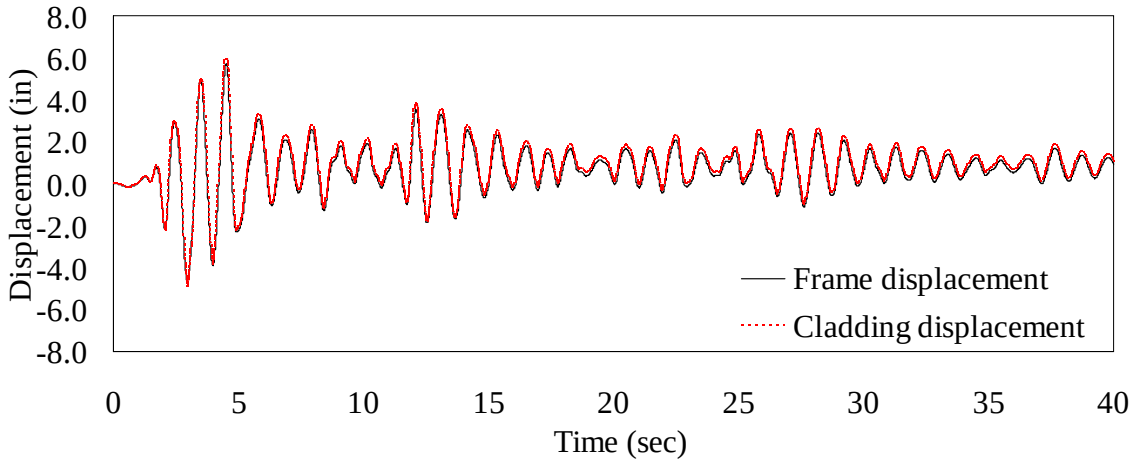

Figure 5.15 Frame and cladding absolute displacements at 3rd floor when tapered tube connections were used.

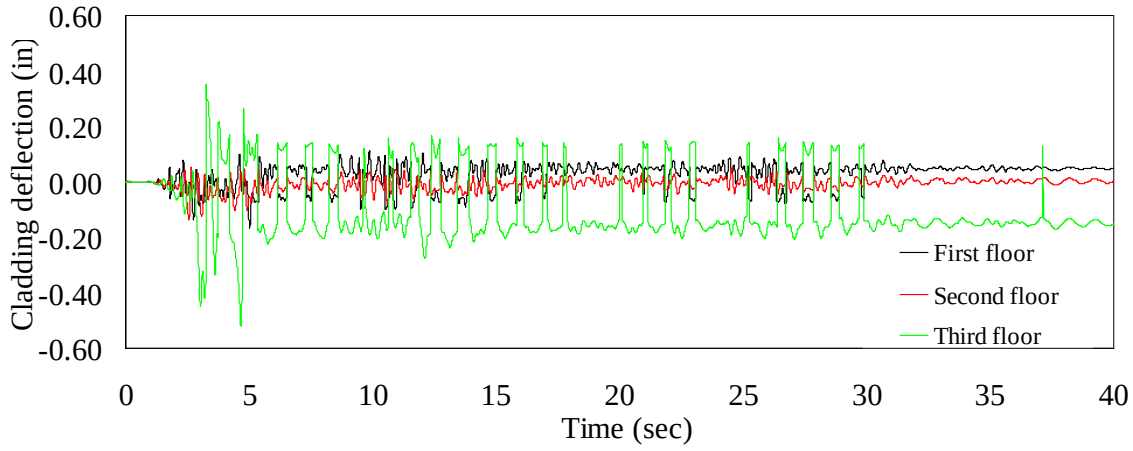

Figure 5.16 Cladding deflection at different floors when tapered tube connections were used.

A range of connection hysteretic behaviors were subsequently modeled to obtain earlier yielding and varying levels of energy dissipation within connections. Hysteretic behaviors with lower yielding stresses were tried to attain more hysteretic damping in connections. Hysteretic behaviors with higher hardening effects were tried to reduce deflection in connections after yielded. "Steel 02" material constitutive law was also used to model these behaviors. Parameters of material model and the corresponding hysteretic behaviors are shown in Table 5.5 and Figure 5.17 - 5.21.

Table 5.5 Parameters of modified hysteretic behaviors.

Parameter set	HLOOP1	HLOOP2	HLOOP3	HLOOP4	HLOOP5
Fy (ksi)	46	46	46	46	46
E (ksi)	4000	4000	4000	4000	4000
b	0.006	0.05	0.1	0.1	0.2
R0	35	35	100	100	150
cR1	0.925	0.925	0.925	0.925	0.925
cR2	0.1	0.1	0.1	0.1	0.1
Cross-sectional area (in^2)	0.04	0.04	0.04	0.06	0.03

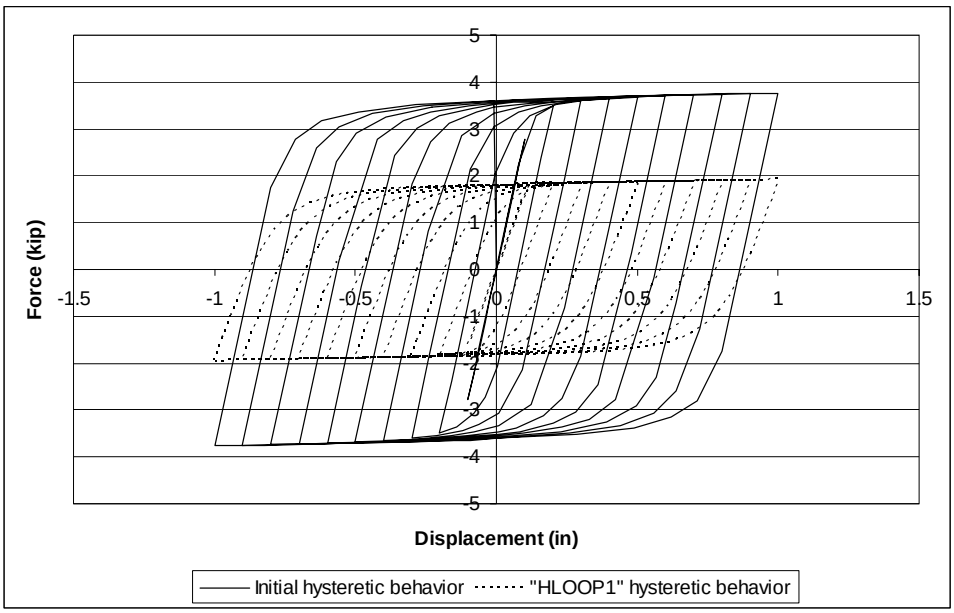

Figure 5.17 Modified hysteretic behavior "HLOOP1".

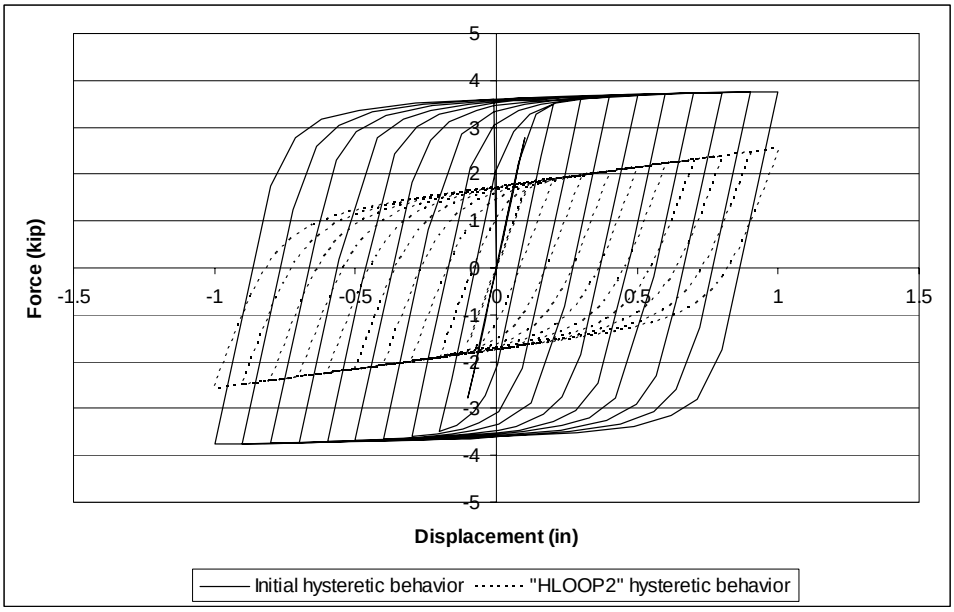

Figure 5.18 Modified hysteretic behavior "HLOOP2".

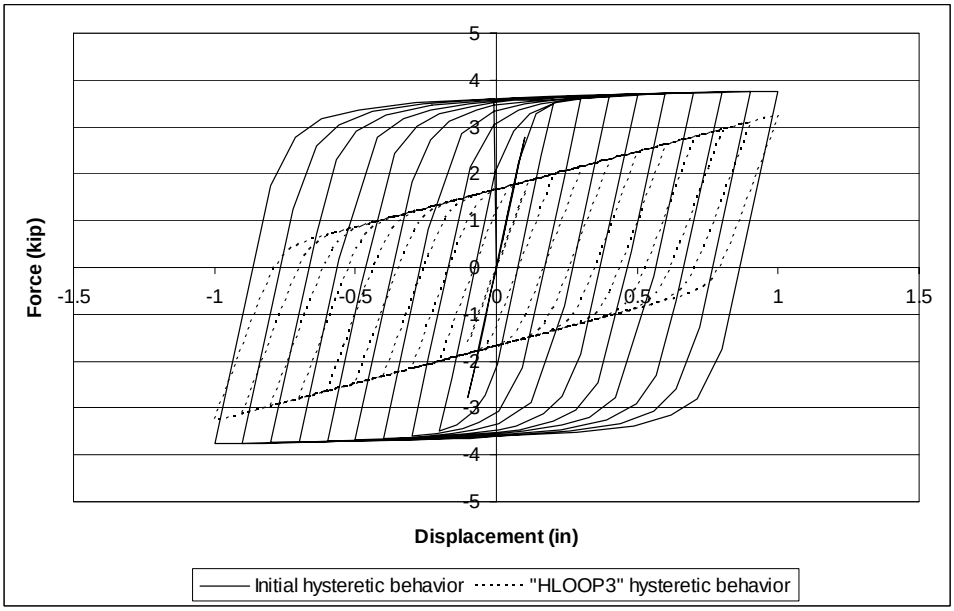

Figure 5.19 Modified hysteretic behavior "HLOOP3".

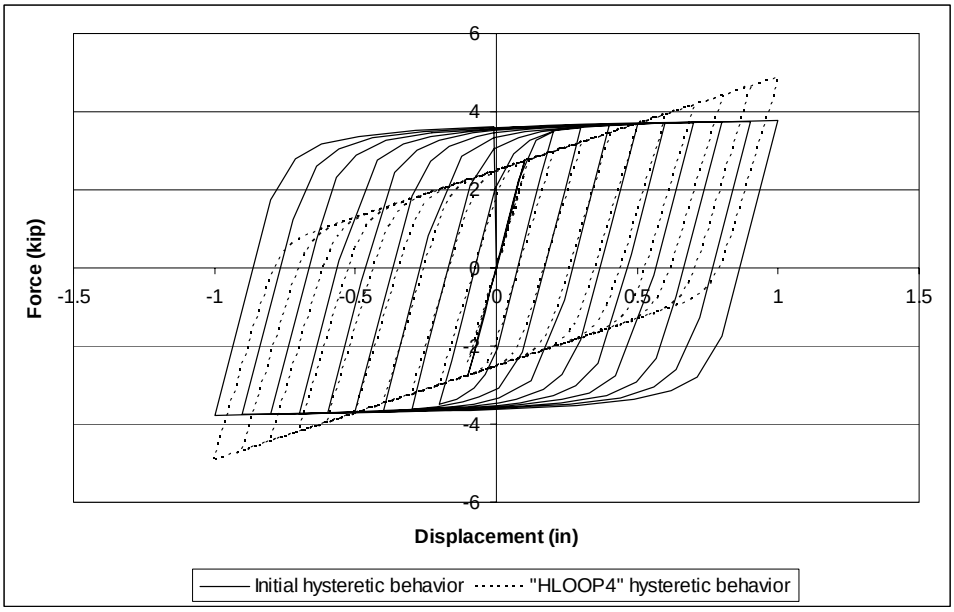

Figure 5.20 Modified hysteretic behavior "HLOOP4".

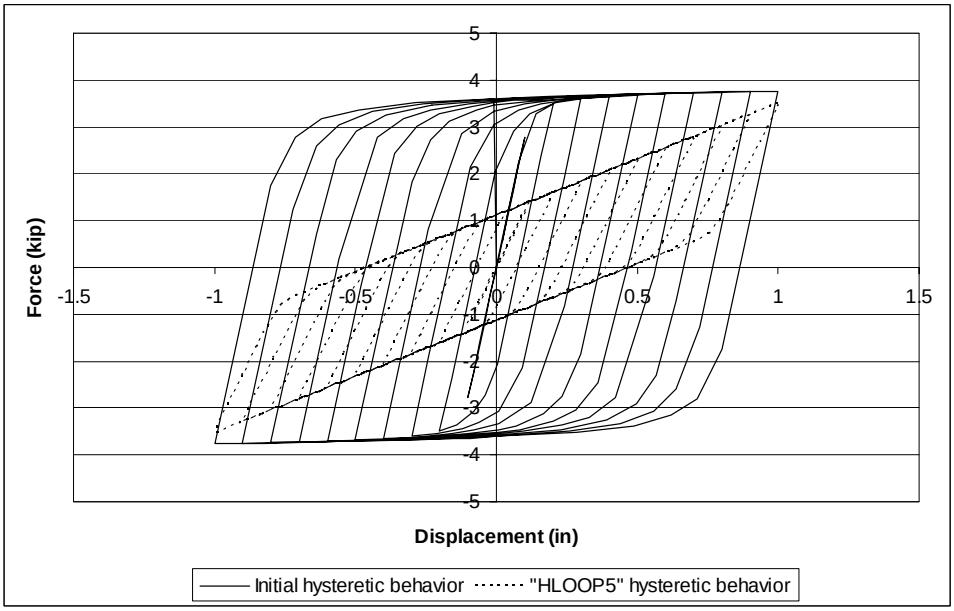

Figure 5.21 Modified hysteretic behavior "HLOOP5".

Analysis results of the reference frame with these modified hysteretic behaviors of connections were shown in Table 5.6. For the case of "HLOOP2", peak story drift

(which occured at the 2nd floor) and base shear were reduced by 10.6% and 4.1% respectively, comparing with the rigid connection case. Time history plots of absolute cladding displacements and absolute frame displacements at 3rd floor for this case were shown in Figure 5.22. Cladding deflections at different floors were shown in Figure 5.23. Larger connection deflections were observed, leading to higher yielding within connections and more effective energy dissipation. However, the connection deflections differed significantly at each floor. The maximum connection deflection was 7 in (0.18 m), which occurred at the 3rd floor, with minimal energy dissipation at the connections on other floors. It is predicted that a more uniform distribution of energy dissipation in the connections, which may provide smaller maximum connection deflection but adequate deflections in all connections will be more effective.

Figure 5.24 shows relative displacements between panels at the 3rd floor. These displacements were measured as the relative displacements between cladding masses in the analysis model. It is noted that the width of gaps between cladding panels was moderate (maximum gap was on the order of 0.64 in (16.3 mm).

Table 5.6 Structural responses when modified hysteretic behavior used.

Structural Responses	Rigid connection	Tapered connection	HLOOP1	HLOOP2	HLOOP3	HLOOP4	HLOOP5
Peak story drift ratio	0.0142	0.0141	0.0134	0.0127	0.0135	0.0139	0.0138
Peak level acceleration (in/s^2)	285.5	283.2	281.3	278.8	280.7	280.4	281.9
Peak base shear (kip)	1116.5	1108.1	1106.5	1070.3	1082.1	1096.8	1088.3
Peak connection deflection (in)	-	0.52	5.51	7.04	2.3	1.3	1.9

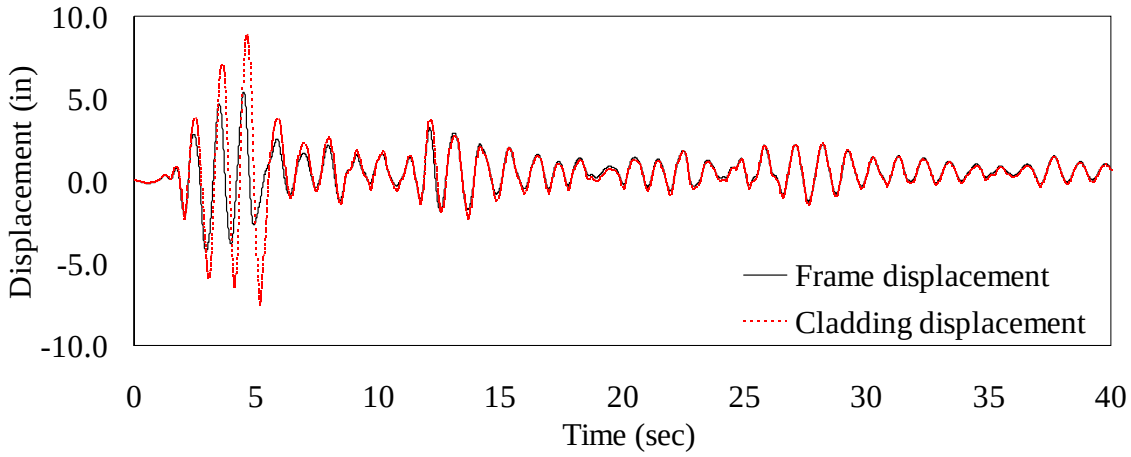

Figure 5.22 Frame and cladding absolute displacements at 3rd floor when "HLOOP2" hysteretic behavior of connections was used.

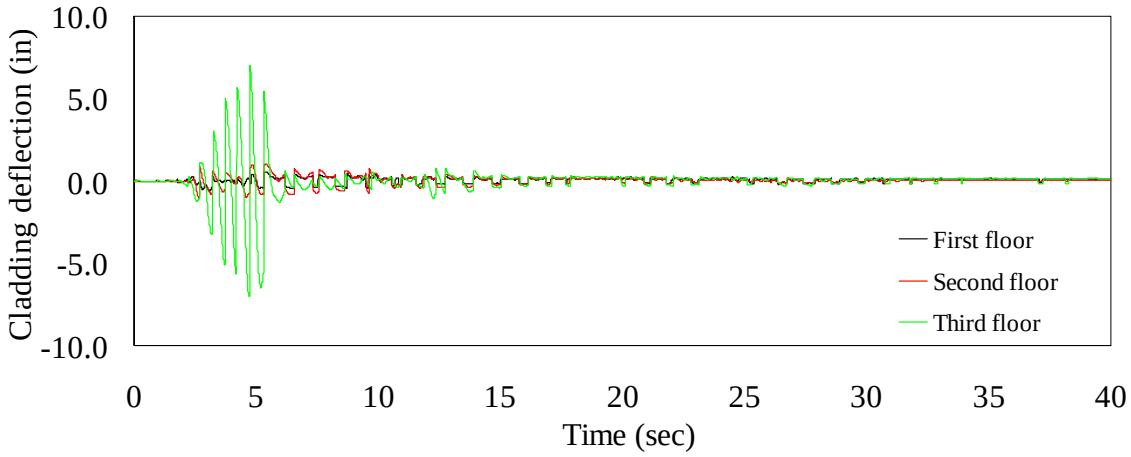

Figure 5.23 Cladding deflection at different floors when "HLOOP2" hysteretic behavior of connections was used.

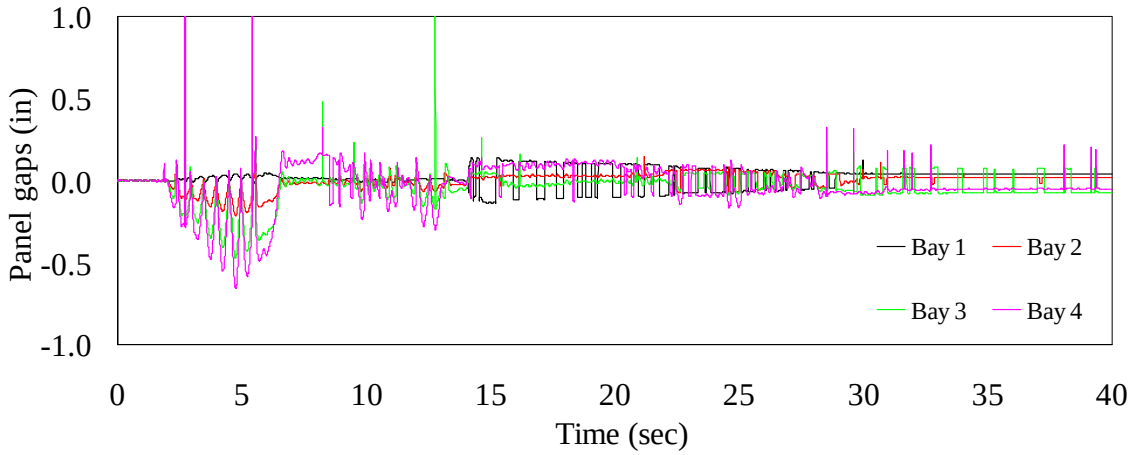

Figure 5.24 Panel gaps due to relative displacement of cladding panels at 3rd floor when "HLOOP2" hysteretic behavior of connections was used.

5.5 Conclusion

This analysis has demonstrated the potential to utilize hysteretic energy dissipation connections to reduce responses of structures under earthquakes. This mechanism with current hysteretic behavior included for connections provides less energy dissipation than the mechanism presented in Chapter 3, but is predicted to require less displacements of cladding. Further analysis including other characteristics of potential connection behavior is needed to obtain more efficient energy dissipation effects.

CHAPTER 6

CONCLUSIONS AND RECOMMENDATIONS

6.1 Summary and conclusions

The objective of this research was to define a methodology for evaluating connection performance and highlight potential benefits and areas needing further study. This research focused on two possible sources of seismic energy dissipation from cladding system connections. First, cladding panels and their connections could incorporate an elastic damping system distributed throughout the building. An analytical model of a SAC 3-story moment resisting frame building including cladding masses and cladding-to-frame connections was developed in SAP2000. Modal analysis results indicated that natural periods and modal participations of the structural frame changed as stiffness of cladding-to-frame connections varied. This change was significant when the stiffness of cladding-to-frame connections in a range where period of cladding units was similar to the fundamental period of the structural frame. It is seen that cladding systems have considerable influences on dynamic behavior of buildings. These influences should be considered in dynamic analysis and designs of structures. Cladding systems may have positive contributions to the behavior of structures when subjected to dynamic loads.

Seismic analysis of elastic systems was performed with earthquake loads including the El Centro earthquake ground motion acceleration, the IBC 2000 design response spectrum and the BOCA 1996 design response spectrum. Reponses of the structural frames were recorded as connections stiffness was varied. Results indicated that base shear and maximum moments in critical structural elements were reduced as much as 40% and 28% respectively comparing with the case of using traditional rigid

connections. Seismic structural responses were reduced the most when natural periods of cladding units were similar to the fundamental period of the frame.

Even though displacement of cladding panels was not controlled with the simplistic connections used in the analysis, the potential to utilize cladding systems as elastic distributed damping systems to dissipate seismic energy was shown. Some initial attempts to limit deflections were also presented. Cladding systems may have the ability to reduce the response of structures under earthquakes if they are designed for this purpose.

The other mechanism to dissipate seismic energy was based on hysteretic damping of cladding-to-frame connections. Promising results reported in previous research were revisited and applied in the reference structure used in this research. Hysteretic behavior of different types of connections was obtained through non-linear analysis of 3-dimensional FEM using ANSYS. Analytical results were calibrated with previously reported experimental results. It was observed that hysteretic response of a connection under cyclic displacements is dependent on rotational conditions at the cladding end of the connection.

Hysteretic behavior of connections obtained from ANSYS analysis were then input into a non-linear frame model of the reference structure developed in OPENSEES. The OPENSEES frame model was able to take into account both geometric and material non-linearity and include hysteretic response of connections. Connections were represented by non-linear springs. Non-linear stiffness of a non-linear spring was defined such that when the spring was subjected to the same load as the connection in the FEA model an equivalent hysteretic response can be obtained. Time history analysis was

performed with the El Centro earthquake ground motion previously used for the SAP2000 model. Resulting response of the structure indicated that initial trial connections were less effective at reducing structural energy demands. The connection stiffness was initially too high to be effective. A range of connection hysteretic behaviors were subsequently modeled to obtain earlier yielding and varying levels of energy dissipation within connections. One hysteretic model resulted in a 10.6% reduction in story drift comparing with the case of using traditional rigid connections. This mechanism with current hysteretic behavior included for connections provides less energy dissipation than an elastic system, but is predicted to require less displacements of cladding. Displacement of cladding and effectiveness of energy dissipation in this mechanism can be improved by using an appropriate hysteretic behavior. For example, incorporating a hysteretic behavior with more hardening, which was not implemented in this research, might help to reduce the displacement of cladding.

6.2 Limitations and recommendations for further research

The current research was only a preliminary investigation of the potential to utilize cladding systems and engineered cladding to structure connections to reduce seismic structural response. Thus, there are aspects in this research that can be improved in further studies. First, in the SAP2000 model, unsophisticated connections which were simply plates of steel were used. At each node, there was only one connection. Rotation at the end of a connection was free. This might not exactly represent the behavior of cladding systems. Even though these limitations did not exist in the OPENSEES model, a better model in SAP2000 to examine the effectiveness of using cladding systems as elastic distributed damping systems should be constructed. More sophisticated

connections which provide equivalent stiffness as used in the current SAP2000 model but result in less displacement of cladding are desired. This is not a simple problem and might require an intensive research related to using different materials as well as innovative configurations of the connections to incorporate additional mass (such as a portion of the floor system) in the pre-cast element.

Using non-linear springs to incorporate hysteretic behavior of connections into the model of the structural frame is convenient and reliable. However, these springs can not support the dead load of cladding. Not all types of hysteretic behavior of connections were modeled in the analysis. This can be improved by employing other material constitutive laws available in OPENSEES. Combining of different available material constitutive laws or developing a new one to represent hysteretic behavior of connections is feasible in OPENSEES. Other hysteretic behavior of connections should be applied to find the most appropriate one for this structure.

After a most effective assumed behavior of connections is realized in OPENSEES, ANSYS analysis could then be re-evaluated with the multiple material models or significant variations to the ones used in this research to find a potential connection. Physical testing of the connection and cladding would verify the boundary conditions modeled and therefore the ANSYS modeling.

Effectiveness of cladding systems is dependent on the dynamic characteristics of the structural frame and the earthquake load applied. Therefore, the concepts need to be investigated with different types of buildings subjected to a range of earthquakes having different characteristics of predominant frequency, peak ground acceleration, duration, input energy, etc. When the structure is subjected to low or moderate magnitude

earthquakes, the first mechanism (MTMD) could be employed. Elastic deformation of connections might be adequate to dissipate seismic energy and reduce structural response. When the structure is subjected to larger earthquakes, hysteretic damping through yielding in the connections could be employed to dissipate seismic energy. A combination of the two mechanisms in the same cladding connection system could also be considered.

BIBLIOGRAPHY

Abe, M., and Fujino, Y. (1994), "Dynamic characterization of multiple tuned mass dampers and some design formulas. Earth-quake engineering and structural dynamics", 23(8), 813-835.

ANSYS Release 11.0, ANSYS, Inc., Program and Help Documentation.

Bruneau, M., and Cohen, J. M. (1994), "Review of NBCC earthquake-resistant design requirements for cladding connectors." Canadian journal of civil engineering, 21(3), 455-460.

Chopra, A. K. (2006), "Dynamics of structures: theory and applications to earthquake engineering." 3rd ed., Prentice Hall, Upper Saddle River, New Jersey.

Clough, R. W., and Penzien, J. (1993), "Dynamics of structures", 2nd ed., McGraw-Hill, New York.

Cohen, J. M. (1995), "Seismic performance of cladding responsibility revisited" Journal of performance of constructed facilities, ASCE, 9(4), 254-270.

Cohen, J. M., and Powell, G. H. (1993), "A design study of an energy-dissipation cladding system." Earthquake engineering and structural dynamics, 22(7), 215-228.

Craig, J., Goodno, B., Pinelli, J.-P., and Moor, C. (1992), "Modeling and evaluation of ductile cladding connection systems for seismic response attenuation in buildings." Proceedings of the 10th World Conference on Earthquake Engineering., A.A. Balkema, Rotterdam, The Netherlands, Vol. 7, 4183-4188.

Goodno, B., El-Gazairly, L., and Hsu, C.-C. (1992), "Use of advanced cladding systems for passive control of building response." Proceedings of the 10th World Conference on Earthquake Engineering., A.A. Balkema, Rotterdam, The Netherlands, Vol. 7, 4195-4200.

Goodno, B. and Palsson, H. (1986), "Analytical studies of building cladding." Journal of structural engineering, ASCE, 112(4), 665-676.

Henry, R.M., and Roll, F. (1986), "Cladding-frame interaction" Journal of structural engineering, ASCE, 112(4), 815-834.

Igusa, T., and Xu, K. (1994), "Vibration control using multiple tuned mass dampers." Journal of sound and vibration, 175(4), 491-503.

Kargahi, M., and Anderson, J. C. (2006), "Structural weight optimization of frames using tabu search. II: Evaluation and seismic performance." Journal of structural engineering, ASCE, 132(12), 1869-1879.

Kargahi, M., Anderson, J. C., and Dessouky, M. M. (2006), "Structural weight optimization of frames using tabu search. I: Optimiztion procedure." Journal of structural engineering, ASCE, 132(12), 1858-1868.

Memari A. M. (2003), "Seismic design of precast concrete cladding panels considering the effect of vertical ground acceleration." Proceedings of the 2003 structures congress and exposition, Structural Engineers' Association of Washington, Seatle, Washington, pp. 913-914.

Memari A. M., Maneetes, H., and Bozorgnia, Y. (2004), "Study of the effect of near-source vertical ground motion on seismic design of precast concrete cladding panels." Journal of architectural engineering, ASCE, 10(4), 167-184.

Neuenhofer, A., and Filippou, F. C., (1998), "Geometrically nonlinear flexibility-based frame finite element." Journal of structural engineering, ASCE, 124(6), 704-711.

Ohtori, Y., Christenson, R.E., Spencer, B.F., and Dyke, S. J. (2004), "Benchmark control problems for seismically excited nonlinear buildings." Journal of Engineering Mechanics, ASCE, 130(4), 366-385.

OpenSees Command Language Manual. Open System for Earthquake Engineering Simulation - Home Page. Sept. 2006. University of California at Berkeley. 25 Feb. 2009. <http://opensees.berkeley.edu/OpenSees/manuals/usermanual/index.html>.

Palsson, H., Goodno, B., Craig, J., and Will, K. (1984), "Cladding influence on dynamics response of tall buildings." Earthquake engineering and structural dynamics, 12(2), 215-228.

Pinelli, J.-P., Craig, J., and Goodno, B. (1990), "Development and experimental calibration of selected dynamic models for precast cladding connections" Proceddings of the fourth U.S. National Conference on Earthquake Engineering, Palm Springs, California, Vol 2., 147-156.

Pinelli, J.-P., Craig, J., and J., Goodno, B. (1995), "Energy-based seismic design of ductile cladding systems." Journal of structural engineering, ASCE, 121(3), 567-578.

Pinelli, J.-P., Craig, J., Goodno, B., and Hsu, C.-C. (1993), "Passive control of building response using energy dissipating cladding connections." Earthquake spectra, 9(3), 529-546.

Pinelli, J.-P., Moor, C., Craig, J., and Goodno, B. (1992), "Experimental testing of ductile cladding connections for building facades." The structural design of tall buildings, Vol. 1, 57-92.

Pinelli, J.-P., Moor, C., Craig, J., and Goodno, B. (1996), "Testing of energy dissipating cladding connections." Earthquake engineering and structural dynamics, 25(2), 129-147.

Precast/Prestressed Concrete Institute (2007), "Architectural precast concrete manual", 3rd ed., Chicago, Illinois.

Reinhorn, A., Soong, T., Lin, R., and Wang, Y. (1989), "1/4 Scale model studies of active tendon systems and active mass dampers for seismic protection." NCEER Report No.89-0026.

Uang, C. M., and Bertero, V. V. (1990), "Evaluation seismic energy in structures." Earthquake engineering and structural dynamics, 19(1), 77-90.

Wang, M. L. (1987), "Cladding performance on a full scale test frame." Earthquake Spectra, 3(1), 119-173.

Wong, K. K. F. (2008), "Seismic Energy Dissipation of inelastic structures with tuned mass dampers." Journal of structural engineering, ASCE, 134(2), 163-172.

Xu, K., and Igusa, T. (1992), "Dynamic characteristics of multiple substructures with closely spaced frequencies." Earthquake engineering and structural dynamics, 21(12), 1059-1070.